Journal of Psychiatric Research 118 (2019) 44–65

Contents lists available at ScienceDirect

Journal of Psychiatric Research

journal homepage: www.elsevier.com/locate/jpsychires

mRNA and miRNA profiles in the nucleus accumbens are related to fear memory and anxiety induced by physical or psychological stress

Kaixin Du[a], Wei Lu[a,**], Yan Sun[a], Jing Feng[a], Jin-Hui Wang[a,b,c,*]

[a] Qingdao University, School of Pharmacy, Qingdao, Shandong, 266021, China
[b] University of Chinese Academy of Sciences, Beijing, 100049, China
[c] Institute of Biophysics, Chinese Academy of Sciences, Beijing, 100101, China

ARTICLE INFO

Keywords:
Fear memory
Anxiety
Neuron
Stress and nucleus accumbens

ABSTRACT

Anxiety is presumably driven by fear memory. The nucleus accumbens involves emotional regulation. Molecular profiles in the nucleus accumbens related to stress-induced fear memory remain elucidated. Fear memory in mice was induced by a paradigm of social defeat. Physical and psychological stress was delivered to an intruder that was attacked by an aggressive resident. Meanwhile, an observer experienced psychological stress by seeing aggressor attacks. The nucleus accumbens tissues from intruder and observer mice that appear fear memory and anxiety as well as control mice were harvested for analyses of mRNA and miRNA profiles by high throughput sequencing. In the nucleus accumbens of intruders and observers with fear memory and anxiety, genes encoding AdrRα, AChRM2/3, GluRM2/8, HrR1, SSR, BDNF and AC are upregulated, while genes encoding DR3/5, PR2, GPγ8 and P450 are downregulated. Physical and/or psychological stress leads to fear memory and anxiety likely by molecules relevant to certain synapses. Moreover, there are differential expressions in genes that encode $GABAR_A$, 5-HTR1/5, CREB3, AChRM2, RyR, Wnt and GPγ13 in the nucleus accumbens from intruders versus observers. GABAergic, serotonergic and cholinergic synapses as well as calcium, Wnt and CREB signaling molecules may be involved in fear memory differently induced by psychological stress and physical/psychological stress. The data from analyzing mRNA and miRNA profiles are consistent. Some molecules are validated by qRT-PCR and dual luciferase reporter assay. Fear memory and anxiety induced by the mixture of physical and psychological stress or psychological stress appear influenced by complicated molecular mechanisms in the nucleus accumbens.

1. Introduction

Fear memory and anxiety often occur in stressful life (Baldi and Bucherelli, 2015; Izquierdo et al., 2016; Makkar et al., 2010). Stresses from physical and/or psychological injuries in individuals can induce fear memory and even depression or anxiety, such as posttraumatic stress disorder and phobia to specific event or objects (Coutellier and Usdin, 2011; Desmedt et al., 2015; Orsini and Maren, 2012; Parsons and Ressler, 2013; Si et al., 2018). Long-term affective disorders often induce secondary diseases in cardiovascular and immune systems (Thrall et al., 2007). It is vital to elucidate cellular and molecular mechanisms underlying the correlation among stress, fear memory and emotional disorders. In general, acute severe stress induces anxiety, while chronic mild stress leads to depression (Overstreet, 2012; Southwick and Charney, 2012; Sun et al., 2018; Willner et al., 1987; Zhu et al., 2017). The erasing of fear memory or memories to negative outcomes is an essential step to diminish pathological emotions and to treat secondary diseases (Wang, J.H., 2019b). Efforts to achieve this goal remain not successful (de Quervain et al., 2017; Flores et al., 2018; Maren, 2011; Sandkuhler and Lee, 2013; Wang, J.H., 2019b). Various types of stresses, such as acute severe stress versus chronic mild stress, psychological stress versus physical stress, and social stress versus natural hazard stress, may induce certain differential cellular and molecular changes in the brain for the suffering of anxiety, depression or their mixture (Ma et al., 2016b; Sutoo and Akiyama, 2002; Xu et al., 2015; Zhang et al., 2012). Comprehensive molecular profiles in relevance to different stresses and their consequences need be addressed for understanding the pathogenesis of these mood disorders and for developing their therapeutic strategies, though certain molecules have been identified (Bagot et al., 2016; Cestari et al., 2014; Johansen et al., 2011;

* Corresponding author. University of Chinese Academy of Sciences, Institute of Biophysics, 15 Datun Road, Chaoyang District, Beijing, 100101, China.
** Corresponding author. Qingdao University, School of Pharmacy, 38 Dengzhou, Qingdao, Shandong, 266021, China.
E-mail addresses: luwei@qdu.edu.cn (W. Lu), jhw@ibp.ac.cn, wangjinhui@ucas.ac.cn (J.-H. Wang).

https://doi.org/10.1016/j.jpsychires.2019.08.013
Received 15 March 2019; Received in revised form 7 August 2019; Accepted 26 August 2019

Kyrke-Smith and Williams, 2018; Otis et al., 2015). In addition, many brain regions have been presumably involved in fear memory, anxiety and depression (Baldi and Bucherelli, 2015; Herry and Johansen, 2014; Wang and Cui, 2017, 2018). Comprehensive molecular profiles in different brain areas relevant to fear memory and anxiety induced by physical and/or psychological stresses should be addressed.

In addition to the amygdala and prefrontal cortex (Ehrlich et al., 2009; Fanselow and Gale, 2003; Garrett and Chang, 2008; Hastings et al., 2004; Keele, 2005; Lebow and Chen, 2016; Lee et al., 2017; Price, 2003), the nucleus accumbens is thought to be an important structure to regulate emotional reaction and cognitive processes (Floresco, 2015; Haruno et al., 2014; Monk et al., 2008; Tzschentke and Schmidt, 2000). Structural elements and functional activities in neuronal circuits including the nucleus accumbens are involved in reward memory versus fear memory (Fadok et al., 2010; Hikida et al., 2016; Ikemoto, 2007; Kochenborger et al., 2012; Russo et al., 2010; Thomas et al., 2002; Yang and Liang, 2014). The abnormality of the nucleus accumbens may lead to anxiety disorders (Anderson et al., 2018; Barrot et al., 2005; Fu et al., 2017; Heshmati et al., 2016; Levita et al., 2012). Some cellular processes and signaling molecules in the nucleus accumbens are presumably involved in anxiety and major depression (Bosch-Bouju et al., 2016; Feng et al., 2017; Francis and Lobo, 2017; Kim et al., 2008; Lim et al., 2012; Monk et al., 2008; Salamone et al., 2005; Si et al., 2018; Zhu et al., 2017). Thus, comprehensive molecular profiles in the nucleus accumbens associated with fear memory and anxiety evoked by the stressful situations should be addressed. It should be emphasized that mRNAs and miRNAs interact each other, and the expression of mRNAs in cells is influenced by miRNAs, by which the bindings of miRNAs with their dicers will degrade mRNAs and weaken their translations (Afonso-Grunz and Muller, 2015; Beilharz et al., 2010; Dalmay, 2013; Valinezhad Orang et al., 2014). In this regard, the simultaneous analyses of mRNA and miRNA with the consistent results should enable the data be more convincing.

Compared to other types of stressful situations, the social stress is more commonly seen in life (Blanchard et al., 2001; Ganzel et al., 2010; Sandi and Haller, 2015). With high level or persistent stress, individuals frequently retract from social interactions or become irritable and anxiety (Sandi and Haller, 2015). Molecular profiles relevant to social stresses from physical injury and psychological injury and its consequences need be addressed. To reach this goal, an animal model of social defeat in resident/intruder paradigm is used (Berton et al., 2006; Bjorkqvist, 2001; Hammels et al., 2015; Martinez et al., 1998; Tsankova et al., 2006; Vasconcelos et al., 2015). In the comparison with the stress induced by electrical stimulations, physical and psychological stress in social interactions may be more close to the real life (Martinez et al., 1998; Tsankova et al., 2006; Vasconcelos et al., 2015). In order to mimic psychological stress only, an observer was placed around to perceive attacks of resident CD1 mouse to an intruder mouse. Therefore, cellular and molecular profiles in the nucleus accumbens relevant to fear memory and anxiety induced by psychological stress and/or physical stresses will be our research focus since it remains not to be systemically investigated. It is noteworthy that many studies have been focused on genetics of stress-relevant disorders as well as genetical factors relevant to vulnerability to stresses and disorder occurrence (Ma et al., 2016a, 2016b; Smoller, 2016; Sun et al., 2018). How social stress induces epigenetic changes, such as miRNAs that interact and regulate mRNA and protein expressions, needs to be investigated.

To molecule profiles in the nucleus accumbens relevant to fear memory and anxiety induced by physical or psychological stress, our strategies are presented below. Two groups of C57 mice were subject to psychological stress only and physical/psychological stress, respectively. Another group was control mice that were given any stress In the mouse model of social defeat, physical and psychological stresses to each of intruder mice were given by attacks from CD1 resident aggressor mice. Psychological stress only to each of observers was achieved by watching this attack. After the treatments for five days, each mouse was examined in a social interaction cage to measure fear memory and an elevated plus maze to assess anxiety state. If mice express fear memory and anxiety, tissues of their nucleus accumbens were harvested within less than 24 h mRNA and microRNA profiles were analyzed by high-throughput sequencing from control mice and fear memory mice induced by physical/psychological stresses or psychological stress only. By joint analyses and comparisons of mRNAs and microRNAs, we expect to figure out inclusive molecular profiles and signaling pathway networks in the nucleus accumbens related to fear memory by social physical and psychological stress. Through this analysis, we also expect to develop new therapeutic strategies.

2. Materials and methods

All experiments were conducted in accordance with the guideline and regulation by Administration Office of Laboratory Animals at Beijing China. Protocols were approved by Institutional Animal Care and Use Committee in this office (B10831). In terms of living condition for normal life and control group, mice were housed in cages (32 × 16 × 16 cm) with free access water and food pellets under. The circadian was 12 h in the light (7:00 a.m.–7:00 p.m.) and the rest of 12 h in the dark. Ambient temperature was 22 ± 2 °C. Relative humidity were 55 ± 5%. These conditions were set in the specific pathogen free (SPF).

Fear memory induced by physical and psychological stresses in mice: The induction of fear memory and anxiety in mice was conducted by social stress in resident/intruder paradigm (Berton et al., 2006; Bjorkqvist, 2001; Golden et al., 2011; Hammels et al., 2015; Martinez et al., 1998; Meerlo et al., 2002; Montagud-Romero et al., 2018; Toyoda, 2017; Tsankova et al., 2006; Vasconcelos et al., 2015). The reason for choosing this model as social stress is due to a fact that physical and psychological stresses during social interactions is more realistic in the life. Electrical stimulation used in other studies is a stressful situation that happen less in real life (Martinez et al., 1998; Tsankova et al., 2006; Vasconcelos et al., 2015). Resident mice in social defeat were male CD1 mice. Aggressive CD1 male mice (also called as aggressors) were selected to be resident mice if the latency of their attacking unfamiliar C57 mice was less than 2 min. Strain C57 male mice were applied for our experiments starting at postnatal week six. The qualified C57 male mice (more active social activity and less anxiety) after experiencing an adaptation week were divided to three groups, or control, intruder and observer. The selection of C57 male mice was based on previous studies, in which male mice or rats have been used (Golden et al., 2011; Hammels et al., 2015). Another reason was to make a situation of more aggressive and offensive in CD1 resident mice when a male intruder was placed into the CD1 resident house and a female CD1 resident was taken out of this house. CD1 male resident mice became more aggressive to attack the intruder mice when a C57 male intruder came in and a female CD1 sexual partner was missed (Goyens and Noirot, 1975). This paradigm made C57 male intruders experienced sufficient physical and psychological stresses (Sun et al., 2019) to become susceptible to and less resilient to anxiety (Golden et al., 2011; Hammels et al., 2015). Intruder and observer C57 mice were selected based on their active social activity and low anxious state (Sun et al., 2019). Their anxious state was examined on the elevated plus maze, and social activity was examined on social interaction cage (please see below). During the adaptation period, these mice allowed to be familiar with cages for their living and social interactions, so that only CD1 resident mice were new to C57 mice in the resident/intruder paradigm for associative learning (Wang, J.-H., 2019). Mice receiving physical attacks from male CD1 residents were called as intruders whose fear memory was induced by physical and psychological stresses through multiple sensory modalities. Mice that viewed these attacks through a transparent partition in the middle of the cage were defined as observers, whose fear memory was induced by psychological stress mainly through the visual system.

In seven days of adaptation period, male CD1 resident mouse and female CD1 mouse that were presumably sexual partner were placed in a room space (29 × 17.5 × 12.5 cm) of normal cage. A neighboring room (29 × 17.5 × 12.5 cm) was isolated by transparent partition for the subsequent stay of an observer (C57 mouse) in order to perceive the psychological stress. In this period, C57 mice were placed in a neighboring room of CD1 living room for them to be familiar with CD1 mice. To each of C57 mice before experiencing social defeat paradigm, the self-control values about the ratio of stay time in the interaction zone with the presence of CD1 or C57 mice in a small container to stay time in the interaction zone without CD1 or C57 in this container were also collected in this period. C57 mice that possess this ratio above 0.5, the stay time in open arms of the elevated plus maze above 2%, and consistent values within mean ± 2SD in these measures were selected for our study. These mice with active social activity and less anxiety were divided into groups of control (n = 13), intruder (n = 13) and observer (n = 11).

In subsequent five days for social defeat, two groups of C57 mice (intruder and observer) would experience physical and/or psychological stress. Each of C57 intruder mice was placed into a living house of CD1 resident mice twice in the morning and afternoon, respectively, when male CD1 mouse was present and female CD1 mouse was taken out this living house. The duration for the C57 intruder mouse to stay in the CD1-living house was based on the attack times when CD1 male resident mouse had bitten the C57 intruder mouse five times on his back. In the meantime, another C57 mouse (observer) was placed into a room neighboring to CD1-living house. The CD1-living house and neighboring room were isolated by a transparent partition. In this model, C57 intruder mice were thought of as the experience of physical and psychological stresses by physical attacks and bites, whereas C57 observer mice were thought of as the experience of psychological stress only by watching attacks.

After this social defeat period, C57 mice in the groups of intruder, observer and control were tested in the formation of fear memory. The object of their fear memory was CD1 resident male mice that had attacked C57 mice. The test of fear memory formation was conducted in a social interaction cage that included a container of holding CD1 aggressor or C57 mice (Fig. 1). The identification of fear memory formation in C57 mice was based on their avoidance to the container of holding a CD1 resident male mouse as well as less access to the interaction zone, but not avoidance to the container of holding C57 mice. Values about the ratio of stay time in interaction zone with the presence of CD1 or C57 mice in a small container to stay time in the interaction zone without CD1 or C57 in this container were measured again for the comparison with their self-control before social defeat. The significant reductions of the ratio of stay time in interaction zone with the presence or without CD1 aggressor in the small container before and after social defeat indicate the formation of fear memory in intruder and/or observer mice.

It is noteworthy that intruder, observer and control mice were separately housed in their own cages during the adaptation period, the intervals of social defeat experiments and the tests of fear memory and anxiety. In other words, there are no chances for these mice among intergroups to the direct interaction for the establishment of social behaviors and empathy.

The test of anxiety state: Anxiety-like behaviors in mice treated by stresses or controls were evaluated by an elevated plus maze (EPM), which is described as a validated and classic method to assess the level of anxiety in the rodents (Pellow and Chopin, 1985; Walf and Frye, 2007). The EPM consists of two open arms (30 × 5 cm) opposite to two closed arms (30 × 5 × 15.25 cm). The arms extended from a central platform (5 × 5 cm). The EPM was located 40 cm above the floor. All experiments were performed between 8:00 to 14:00. Mice naturally avoid the open field. On the other hand, they intend to explore a new environment for food. In this regard, the measurement for mice avoiding the open field was the duration when mice stayed in the closed arms, i.e., the duration in the closed arms versus total experimental time, whereas the measurement for mice exploring the new environment was exploration times toward the open arms. Therefore, exploration times and the duration in the open arms were used to evaluate the level of anxiety, which were recorded by an automatic video-tracking system for 5 min. Mice were placed at the central platform of an elevated plus maze with facing to an open arm at the beginning of experiments. High anxiety-like behaviors are described as mice spending more time in the closed arms as well as having lower exploration times toward the open arms (Liu et al., 2014; Zhang et al., 2012).

RNA purification from nucleus accumbens tissues. After confirmed the formation of fear memory by psychological stress in observers versus physical/psychological stress in intruders within 24 h, these mice and control mice were anesthetized by Isoflurane, perfused by 4 °C physiological saline through left atrium and decapitated by a guillotine.

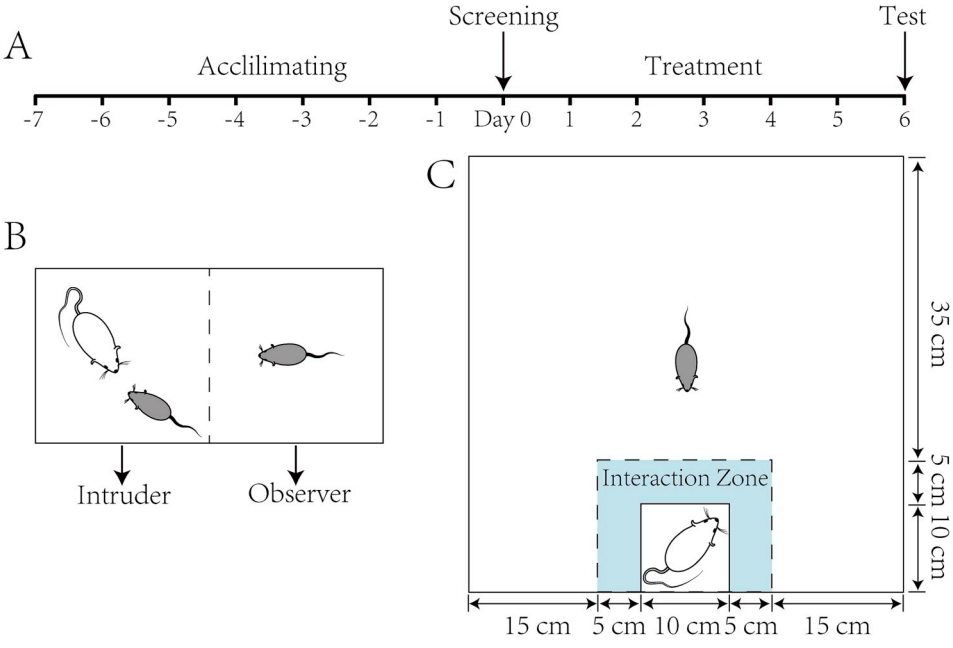

Fig. 1. The schematic of social defeat and social interaction test to the stress induce fear memory mice.
A) After 7-days of acclimation, elevated plus maze (EPM) test and social interaction test were used to screen C57 mice before stress treatments. Stress treatment scheme uses 5-days of consecutive social defeat were performed in the morning and afternoon. Elevated plus maze (EPM) test and social interaction test were used again to test the anxiety and fear memory of C57 mice, followed by gene sequencing. B) Intruder C57 mouse was placed in the CD-1 home cage, physical and psychological stress were performed when the aggressive behavior of the CD-1 mouse was detected; Observer C57 mouse was placed in the cage next to the CD-1 home cage, psychological stress was performed when the observer C57 mouse was able to watch the aggressive behavior of the CD-1 mouse through a transparent sheet between to cages. C) The social interaction test was performed in an open field box (50*50 cm) with a transparent and perforated cage of 10*10 cm on the edge. The area around the small cage was defined as the interaction zone.

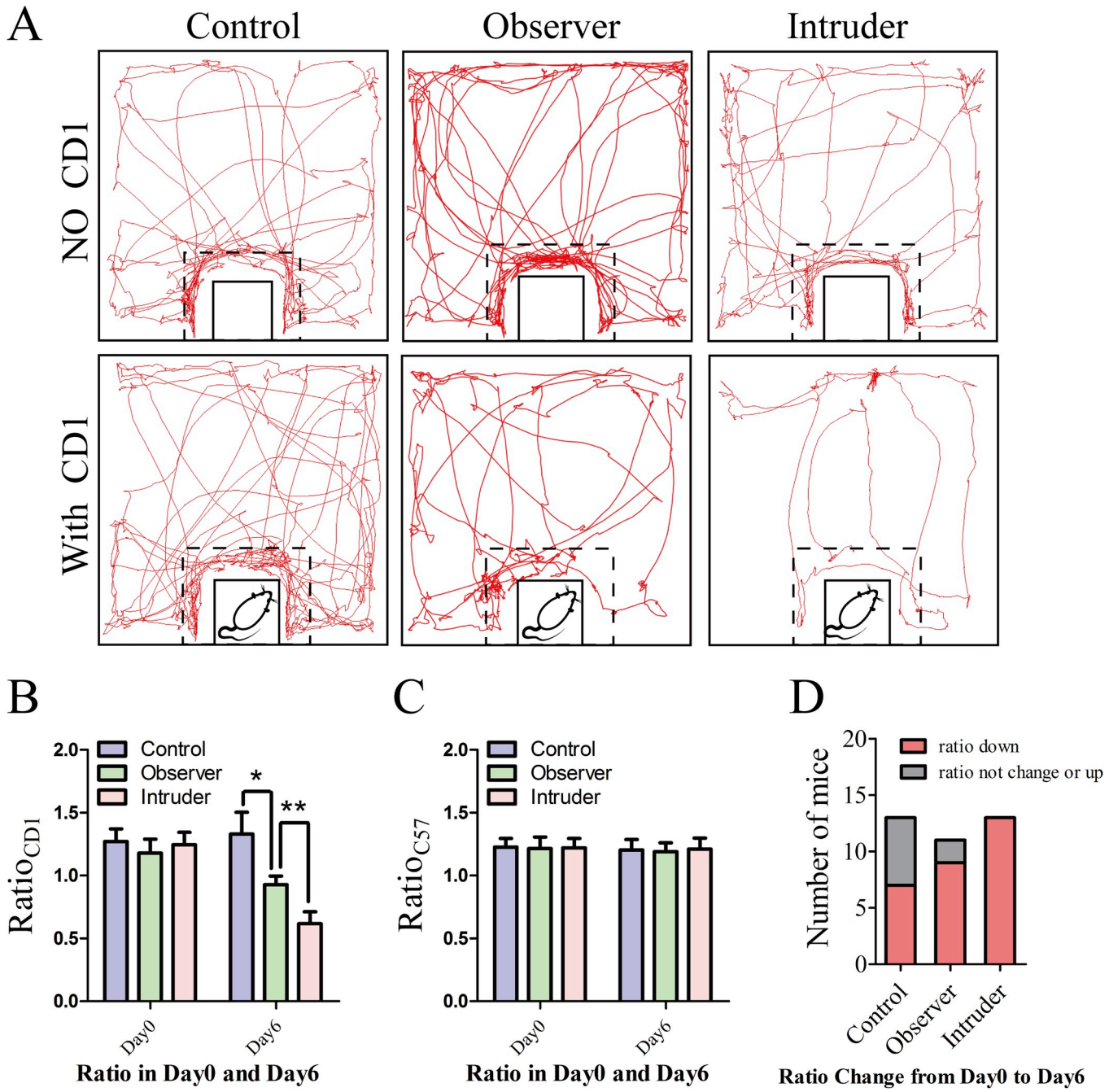

Fig. 2. Stress treatment leads mice to express avoidance behaviors. Control group n = 13, Observer group n = 11, Intruder group n = 13. A) representative motion trajectory of social interaction test for Intruder, Observer and Control mice in Day0 and Day6. B) shows when screen C57, the Ratio values (%) in the mice between Control (blue bar), Observer (green bar) and Intruder (pink bar) group in Day0 and Day6. C) shows when screen CD1, the Ratio values (%) in the mice between Control (blue bar), Observer (green bar) and Intruder (pink bar) group in Day0 and Day6. D) shows the number of mice with Ratio get down (red) or else (gray) from Day0 to Day6, chi-square test was used and p = 0.0190. (For interpretation of the references to colour in this figure legend, the reader is referred to the Web version of this article.)

Both sides of the nucleus accumbens were quickly isolated and dissected on ice-cold glass slide. Total RNAs from the nucleus accumbens of each mouse were isolated by TRIzol Reagent (Life Technologies, Carlsbad, CA, USA; (Ma et al., 2016b);). RNA samples in dry ice were sent to Beijing Genomics Institute (BGI) for high-throughput sequencing. The concentration of total RNAs, the value of RNA integrity number (RIN) and the ratios of 28S to 18S ribosomal RNAs were measured by 2100 Bioanalyzer (Agilent Technology, USA) with RNA 6000 nano Reagents Port 1 for their quality control. Samples with total RNAs larger than 10 μg, the concentration larger than 200 ng/μl, the RIN larger than 8, and the ratio of 28S to 18S larger than 1.5 were chosen for the construction of transcriptome and small RNA libraries. Nucleus accumbens tissues that met these qualifications from each of three mice in groups of control, intrudes and observer were used for high-throughput sequencing with correlation coefficient above 0.8.

RNA sequencing. mRNAs from total RNAs were randomly sheared into 200 bp fragment by oligo (dT) beads. Fragments were reversely transcribed to cDNA by random oligonucleotides. These cDNAs were purified by QiaQuick PCR extraction kit and ligated by sequencing adaptors after end repair. Their amplification was done with Illumina

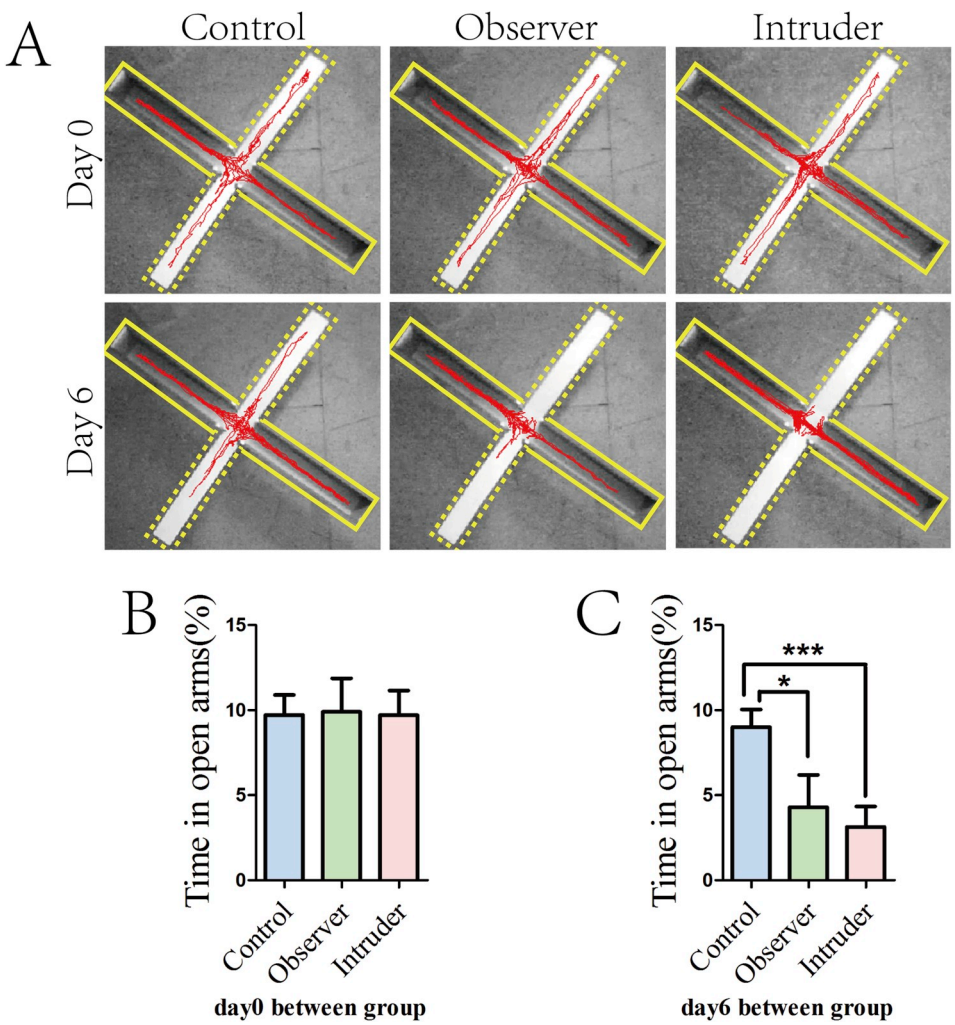

Fig. 3. Stress treatment leads mice to express anxiety behaviors. Control group n = 13, Observer group n = 11, Intruder group n = 13. A) shows the motion trajectory of C57 mice in elevated cross maze before and after stress treatments. B) illustrates the time in open zone (%) of Control group (blue bar), Observer group (green bar) and Intruder group (pink bar) in day0, there is no significant differences between each group in day0. C) illustrates the time in open zone(%) of Control group (blue bar), Observer group (green bar) and Intruder group (pink bar) in day6. One-way ANOVA was used for the comparisons among Intruder, Observer and Control mice, while three asterisks show $p < 0.001$, one asterisks show $p < 0.05$ in which two-sample *t*-test was used for the comparisons between groups. (For interpretation of the references to colour in this figure legend, the reader is referred to the Web version of this article.)

PCR Primer Cocktail in 15 PCR-reaction cycles. After purifying by agarose gel electrophoresis, cDNAs between 200 and 300 bp were used for library construction.

18-30 nt RNAs were isolated from total RNAs by polyacrylamide gel electrophoresis. They were applied to construct microRNA sequencing library. RNAs ligated to 5′-RNA adapter by T4 RNA ligase were size-fractionated and 36–50 nucleotide fractions were excised. The precipitated RNAs were ligated to 3′-RNA adapter by T4 RNA ligase and size-fractionated, and then 62–75 nucleotide fraction (small RNA + adaptors) was excised. To produce the templates enough for the sequencing, small RNAs ligated with adaptors were subjected to RT-PCR. Products were purified and collected by gel purification for high-throughput sequencing.

Qualities of mRNA and microRNA libraries were evaluated by 2100 Bioanalyzer (Agilent Technologies, CA USA). Their quantities were verified by ABI StepOnePlus Real-Time PCR System. Their sequencings were done by Illumina HiseqTM 2500 platform (Illumina Inc., San Diego, CA USA). In two libraries, average reading length were about 100 bp (pair-end) and 49 bp (single-end), respectively.

Bioinformatics for mRNA. Original image data was transformed into raw data or raw reads by base calling. Dynamic Trim Perl script implemented in SolexaQA package was done to control the quality of raw sequencing data. Reads with adapters, unknown bases more than 10% as well as 50% bases with low quality score (PHRED score 5) were removed. The remained “clean reads” were mapped to mouse genome reference sequence (UCSC mm10) by TopHat v1.0.12 incorporated Bowtie v0.11.3 software to perform alignments. The maximum of allowable mismatch was set to three for each read in the alignment and mapping. To calculate gene expression level, sole reads uniquely aligned to genes were used. Reads per kilo-base per million reads (RPKM) were used for gene expression. Genes in low expression level (RPKM < 0.5) were removed for further analysis.

The DEseq2 package method was used to screen differential expressed genes (DEGs) DEGs between two groups with biological replicates, e.g., control versus intruder, control versus observer, intruder versus observer. A threshold to identify DEGs was fold-change above 1.5. Pathway enrichment analysis in DEGs association with physiological or biochemical processes were conducted. Hypergeometric test implemented in tool WebGestalt (version 2) and canonical pathways from Kyoto Encyclopedia of Genes and Genomes (KEGG) database were used in these enrichment analyses. Compared with whole genome background, the enriched metabolic pathways or signal transduction pathways in DEGs would be identified in the analyses. *P*-values in hypergeometric tests were adjusted by Benjamini-Hochberg method. Pathways with adjusted *p*-values less than 0.05 were thought to be significant enrichments.

Bioinformatics for microRNA (miRNA). Adaptor sequences, low-quality reads and contaminant in 49 nt-tags from Hiseq sequencing were removed. The remained credible clean reads were aligned to Genbank database and Rfam database with blast or bowtie softwares to further remove reads of noncoding RNA, such as ribosomal RNAs, transfer RNAs, small nuclear RNAs, small nucleolar RNAs and repeat RNA. To obtain miRNA count, high-quality clean reads ranging in 18–25 nt were matched to the known miRNA precursor of

Table 1
Signaling pathways identified by KEGG based on DEGs data of NAc in Intruder versus Control.

KEGG Entry	Term	count	Genes
mmu04080	Neuroactive ligand-receptor interaction	22	*Cckbr(cholecystokinin B receptor)↑, Ntsr1(neurotensin receptor 1)↑, Sstr2(somatostatin receptor 2)↑, Sstr1(somatostatin receptor 1)↑, Hrh1(histamine receptor H1)↑, Sstr3(somatostatin receptor 3)↑, Chrm3(cholinergic receptor, muscarinic 3, cardiac)↑, Rxfp1(relaxin/insulin-like family peptide receptor 1)↑, Crhr1(corticotropin releasing hormone receptor 1)↑, Grm2(glutamate receptor, metabotropic 2)↑, Grm8(glutamate receptor, metabotropic 8)↑, Adra1b(adrenergic receptor, alpha 1b)↑, Adra1d(adrenergic receptor, alpha1d)↑, Adra2a(adrenergic receptor, alpha 2a)↑, Gabrg1(gamma-aminobutyric acid (GABA) A receptor, subunit gamma 1)↓, Drd3(dopamine receptor D3)↓, Tacr1(tachykinin receptor 1)↓, Grik2(glutamate receptor, ionotropic, kainate 2 (beta 2))↓, P2ry1(purinergic receptor P2Y, G-protein coupled 1)↓, Htr2c(5-hydroxytryptamine (serotonin) receptor 2C)↓, Trhr(thyrotropin releasing hormone receptor)↓, Npy2r(neuropeptide Y receptor Y2)↓,*
mmu04020	Calcium signaling pathway	14	*Tnnc1(troponin C, cardiac/slow skeletal)↑, Hrh1(histamine receptor H1)↑, Adcy8(adenylate cyclase 8)↑, Cacna1g(calcium channel, voltage-dependent, T type, alpha 1G subunit)↑, Chrm3(cholinergic receptor, muscarinic 3, cardiac)↑, Adra1b(adrenergic receptor, alpha 1b)↑, Adra1d(adrenergic receptor, alpha 1d)↑, Plce1(phospholipase C, epsilon 1)↓, Tacr1(tachykinin receptor 1)↓, Htr2c(5-hydroxytryptamine (serotonin) receptor 2C)↓, Trhr(thyrotropin releasing hormone receptor)↓, Pde1c(phosphodiesterase 1C)↓,*
mmu04310	Wnt signaling pathway	8	*Wnt10a(wingless-type MMTV integration site family, member 10A)↑, Wnt9a(wingless-type MMTV integration site family, member 9A)↑, Wnt4(wingless-type MMTV integration site family, member 4)↑, Fzd9(frizzled class receptor 9)↑, Wnt7a(wingless-type MMTV integration site family, member 7A)↓, Sfrp1(secreted frizzled-related protein 1)↓, Fzd4(frizzled class receptor 4)↓, Ccnd1(cyclin D1)↑,*
mmu04727	GABAergic synapse	6	*Gabrg1(gamma-aminobutyric acid (GABA) A receptor, subunit gamma 1)↓, Gls2(glutaminase 2 (liver, mitochondrial))↑, Adcy8(adenylate cyclase 8)↑, Kcnj6(potassium inwardly-rectifying channel, subfamily J, member 6)↑, Gad2(glutamic acid decarboxylase 2)↓, Hap1(huntingtin-associated protein 1)↓,*
mmu04722	Neurotrophin signaling pathway	7	*Bdnf(brain derived neurotrophic factor)↑, Ngf(nerve growth factor)↑ Arhgdig(Rho GDP dissociation inhibitor (GDI) gamma)↑, Mapk11(mitogen-activated protein kinase 11)↑, Sh2b2(SH2B adaptor protein 2)↑, Rps6ka5(ribosomal protein S6 kinase, polypeptide 5)↓, Rps6ka6(ribosomal protein S6 kinase polypeptide 6)↓,*
mmu04360	Axon guidance	7	*Robo3(roundabout guidance receptor 3)↑, Ephb3(Eph receptor B3)↑, Sema7a(sema domain, immunoglobulin domain (Ig), and GPI membrane anchor, (semaphorin)7A)↑, Ntng2(netrin G2)↑, Ntn1(netrin 1)↓ Rnd1(Rho family GTPase 1)↑, Limk1(LIM-domain containing, protein kinase)↑,*
mmu04723	Retrograde endocannabinoid signaling	6	*Kcnj6(potassium inwardly-rectifying channel, subfamily J, member 6)↑, Adcy8(adenylate cyclase 8)↑, Faah(fatty acid amide hydrolase)↑, Mapk11(mitogen-activated protein kinase 11)↑, Slc17a7(solute carrier family 17 (sodium-dependent inorganic phosphate cotransporter), member 7)↑, Gabrg1(gamma-aminobutyric acid (GABA) A receptor, subunit gamma 1)↓,*
mmu05014	Amyotrophic lateral sclerosis (ALS)	4	*Mapk11(mitogen-activated protein kinase 11)↑, Nefm(neurofilament, medium polypeptide)↑, Nefl(neurofilament, light polypeptide)↑, Nefh(neurofilament, heavy polypeptide)↑,*
mmu04724	Glutamatergic synapse	6	*Slc17a7(solute carrier family 17 (sodium-dependent inorganic phosphate cotransporter), member 7)↑, Gls2(glutaminase 2 (liver, mitochondrial))↑, Grm2(glutamate receptor, metabotropic 2)↑, Grm8(glutamate receptor, metabotropic 8)↑, Grik2(glutamate receptor, ionotropic, kainate 2 (beta 2))↓, Adcy8(adenylate cyclase 8)↑,*
mmu04540	Gap junction	5	*Tuba8(tubulin, alpha 8)↑, Adcy8(adenylate cyclase 8)↑, Htr2c(5-hydroxytryptamine (serotonin) receptor 2C)↓, Prkg1(protein kinase, cGMP-dependent, type I)↓, Gucy1a3(guanylate cyclase 1, soluble, alpha 3)↓,*

(*continued on next page*)

Table 1 (*continued*)

KEGG Entry	Term	count	Genes
mmu04725	Cholinergic synapse	5	*Chrm3(cholinergic receptor, muscarinic 3, cardiac)↑, Kcnj6(potassium inwardly-rectifying channel, subfamily J, member 6)↑, Kcnq4(potassium voltage-gated channel, subfamily Q, member 4)↑, Adcy8(adenylate cyclase 8)↑, Slc5a7(solute carrier family 5 (choline transporter), member 7)↓,*
mmu04726	Serotonergic synapse	2	*Htr2c(5-hydroxytryptamine (serotonin) receptor 2C)↓, Kcnj6(potassium inwardly-rectifying channel, subfamily J, member 6)↑,*

Note: ↑ indicates up-regulation in the tissue of Nac from Intruder versus control mice, whereas ↓ represents down-regulation.

corresponding species in miRBase. miRNAs, which were tags aligned to miRNA precursor in miRBase with no mismatch as well as mature miRNA in miRBase with at least 16 nt overlap allowing offset, would be counted to get the expression of identified miRNAs. For the remained reads without any annotation, Miredp was used to predict potential novel miRNAs and its stem loop structure (Friedlander et al., 2012, 2014). To correct biased results from low expression, miRNAs with read counts less than 5 were discarded in differential expression analysis.

DESeq2 software algorithm based on negative binomial distribution and biology duplicate samples was used to compare the known or novel miRNA expression in control versus intruder, control versus observer and intruder versus observer. Threshold used to identify different expression of miRNAs was fold-change larger than 1.5 and *P*-value less than 0.05. Three miRNA target prediction softwares (RNAhybrid, Targetscan and miRanda) were used to predict gene targets of differentially expressed miRNAs.

Integrated miRNA/mRNA network analysis. Bioinformatics analysis was conducted to find correlations between differentially expressed miRNAs and their target mRNAs. miRNAs were negatively correlated with their targeted mRNAs in theory, despite a few exceptions (He et al., 2016). The differentially expressed miRNAs and transcripts were integrated to identify potential miRNA-regulated target genes. 1) miRNAs and mRNAs should be simultaneously and reversely changed in our analyses. 2) mRNAs should be predicted by miRNAs from RNAhybrid, Targetscan and miRanda. Interactive networks from differentially expressed miRNAs and simultaneously expressed target mRNAs were visualized by Cytoscape software (San Diego, CA USA).

Quantitative RT-PCR for the validations of miRNA and mRNA. Quantitative real-time RT-PCR (qRT-PCR) by SYBR Green technique were used to analyze 14 mRNAs and 13 miRNAs that were involved in cell function and significantly different among control mice as well as intruder and observer mice with fear memory. Supplementary Table One (Table S1) presented the used primers. Briefly, real-time PCR was conducted with a Bio-Rad CFX96Touch. Total RNA was extracted from the nucleus accumbens with a TRIzol Kit. cDNA was synthesized by PrimeScript RT Reagent Kit (TaKaRa, RR037A, Kusatsu, Japan) and Mir-X miRNA First-Strand Synthesis Kit (Clontech, 638315, CA, USA) for mRNA and miRNA, respectively. mRNAs were amplified in a 20 μl reaction with 1 μl sample cDNA, 1.5 μl of each primer (0.75 μmol/l), 10 μl 2 × qPCR Mastermix (Green) and 6 μl ddH_2O. Real-time PCR was initiated at 95 °C for 2 min, followed by 40 cycles of denaturation for 5 s at 95 °C, annealing and elongation for 10 s at 60 °C and melt curve 65 °C–95 °C increment 0.5 °C for 5sec. For miRNAs, qRT-PCR was performed in a 20 μl reaction with 2 μl sample cDNA, 0.5 μl mRQ3′Primer, 0.5 μl miRNA-specific Prime (10 μM), 12.5 μl 2 × SYBR Advantage Premix and 9.5 μl ddH_2O. The program was set to 95 °C for 10 s, followed by 40 cycles of denaturation for 5 s at 95 °C, annealing and elongation for 20 s at 60 °C and melt curve 65 °C–95 °C increment 0.5 °C for 5 s. The relative expression level of mRNAs in the tissue was normalized to an internal reference gene GAPDH. The relative expression level of miRNAs in the tissue was normalized to U6 small nucleolar RNA. qRT-PCR runs were repeated in three replications. The results were calculated with the $2^{-\Delta\Delta Ct}$ method (Livak and Schmittgen, 2001).

Dual luciferase reporter assay. The sequence containing the targeted sites of targeted gene was amplified, digested by XhoI/NotI and fused into luciferase vector psiCHECK2 (Ma et al., 2016a, 2016b). The site-directed mutation of the detected miRNA-targeted site was performed with QuikChange Lighting Site-Directed Mutagenesis Kit (Stratagene, La Jolla, CA USA) based on manufacturer's instructions. Luciferase reporter detection assays were conducted as described (Ma et al., 2016b). HEK293T cells were planted at 5×10^4 cells per well in 24-well plates and maintained in DMEM containing 10% FBS. After 24 h, these cells were co-transfected with 50 ng psiCHECK2-wild-type or mutant reporter plasmids, 50 nM miRNAs mimic or miRNA-NC by Lipofectamine 2000 transfection reagent (Invitrogen, Carlsbad, CA USA). After 48 h, activities of firefly and Renilla luciferase were assessed by Dual-Glo® Luciferase Assay System (Promega, Cat. E2920, USA) based on manufacturer guides. Each treatment was done in the triplicates from three independent experiments.

Different expression and biological indication. In the comparisons of the data from the nucleus accumbens between control and intruder, control and observer as well as intruder and observer groups, the 1.5 fold ratio of RPKM values in differential expressions was set as the involvement of stress-induced fear memory. If mRNAs were differentially expressed between control and intruder mice, these mRNAs were presumably associated with fear memory induced by physical/psychological stress. mRNAs that were differentially expressed between control and observer mice were presumably associated with fear memory induced by psychological stress. mRNAs that were differentially expressed between intruder and observe mice were likely associated with fear memory induced by physical stress. If mRNAs were differentially expressed between control and intruder as well as between control and observer, but showed similar expression between intruder and observer, these mRNAs were likely associated with both physical and psychological stresses.

Statistical analyses. By DESeq2 software algorithm, the initial processing raw data of mRNA and miRNA expression profiles were performed, respectively. Data in behavior tests, luciferase activity and gene analyses are presented as mean ± SEM. Relationships between miRNAs and their target prediction were assessed by Pearson's correlation coefficients. The unpaired student t-test was used to make statistic comparison between control and intruder, control and observer, intruder and observer mice in the data of molecular biology. As the data from emotional behavior tasks demonstrates relatively large variation, one-way ANOVA was used to compare data from behavioral tests among groups. Student t-test was used for the comparison of data before and after stress paradigm. In the meantime, two-way repeated ANOVA measures with post-hoc comparison by Student-Newman-Keuls test were used for among groups before and after treatments. $P < 0.05$ values are thought to be statistically significant (Ma et al., 2016a, 2016b).

3. Results

3.1. Fear memory and anxiety induced by physical and/or psychological stresses

When a C57 mice was placed into the home cage of resident CD1

Table 2
Signaling pathways identified by KEGG based on DEGs data of NAc in Observer versus Control.

KEGG Entry	Term	count	Genes
mmu04723	Retrograde endocannabinoid signaling	18	*Slc17a7(solute carrier family 17 (sodium-dependent inorganic phosphate cotransporter), member 7)↑, Slc17a6(solute carrier family 17 (sodium-dependent inorganic phosphate cotransporter), member 6)↑, Gabra3(gamma-aminobutyric acid (GABA) A receptor, subunit alpha 3)↑, Gabra1(gamma-aminobutyric acid (GABA) A receptor, subunit alpha 1)↑, Kcnj3(potassium inwardly-rectifying channel, subfamily J, member 3)↑, Kcnj9(potassium inwardly-rectifying channel, subfamily J, member 9)↑, Kcnj6(potassium inwardly-rectifying channel, subfamily J, member 6)↑, Faah(fatty acid amide hydrolase)↑, Plcb4(phospholipase C, beta 4)↑, Gng2(guanine nucleotide binding protein (G protein), gamma 2)↑, Napepld(N-acyl phosphatidylethanolamine phospholipase D)↑, Adcy1(adenylate cyclase 1)↑, Adcy2(adenylate cyclase 2)↑, Ptgs2(prostaglandin-endoperoxide synthase 2)↑, Mapk11(mitogen-activated protein kinase 11)↑, Adcy8(adenylate cyclase 8)↑, Slc17a8(solute carrier family 17 (sodium-dependent inorganic phosphate cotransporter), member 8)↓, Gng8(guanine nucleotide binding protein (G protein), gamma 8)↓,*
mmu04080	Neuroactive ligand-receptor interaction	28	*Hrh1(histamine receptor H1)↑, Grm2(glutamate receptor, metabotropic 2)↑, Gabra1(gamma-aminobutyric acid (GABA) A receptor, subunit alpha 1)↑, Gabra3(gamma-aminobutyric acid (GABA) A receptor, subunit alpha 3)↑, Adra2a(adrenergic receptor, alpha 2a)↑, Sstr2(somatostatin receptor 2)↑, Cckbr(cholecystokinin B receptor)↑, Mas1(MAS1 oncogene)↑, Chrna4(cholinergic receptor, nicotinic, alpha polypeptide 4)↑, Gabbr2(gamma-aminobutyric acid (GABA) B receptor, 2)↑, Htr5a(5-hydroxytryptamine (serotonin) receptor 5A)↑, Sstr3(somatostatin receptor 3)↑, Nmbr(neuromedin B receptor)↑, Ntsr1(neurotensin receptor 1)↑, Sstr1(somatostatin receptor 1)↑, Rxfp1(relaxin/insulin-like family peptide receptor 1)↑, Crhr1(corticotropin releasing hormone receptor 1)↑, Chrm3(cholinergic receptor, muscarinic 3, cardiac)↑, Chrm2(cholinergic receptor, muscarinic 2, cardiac)↑, Grm8(glutamate receptor, metabotropic 8)↑, Adra1d(adrenergic receptor, alpha 1d)↑, Adra1b(adrenergic receptor, alpha 1b)↑, Tacr1(tachykinin receptor 1)↓, Drd3(dopamine receptor D3)↓, P2ry1(purinergic receptor P2Y, G-protein coupled 1)↓, Trhr(thyrotropin releasing hormone receptor)↓, Lpar6(lysophosphatidic acid receptor 6)↓, Npy2r(neuropeptide Y receptor Y2)↓,*
mmu04020	Calcium signaling pathway	19	*Tnnc1(troponin C, cardiac/slow skeletal)↑, Ryr2(ryanodine receptor 2, cardiac)↑, Cacna1g(calcium channel, voltage-dependent, T type, alpha 1G subunit)↑, Slc8a1(solute carrier family 8 (sodium/calcium exchanger), member 1)↑, Plcb4(phospholipase C, beta 4)↑, Cckbr(cholecystokinin B receptor)↑, Adra1b(adrenergic receptor, alpha 1b)↑, Adcy1(adenylate cyclase 1)↑, Adcy8(adenylate cyclase 8)↑, Ntsr1(neurotensin receptor 1)↑, Hrh1(histamine receptor H1)↑, Adcy2(adenylate cyclase 2)↑, Pde1a(phosphodiesterase 1A, calmodulin-dependent)↑, Htr5a(5-hydroxytryptamine (serotonin) receptor 5A)↑, Chrm3(cholinergic receptor, muscarinic 3, cardiac)↑, Chrm2(cholinergic receptor, muscarinic 2, cardiac)↑, Adra1d(adrenergic receptor, alpha 1d)↑, Trhr(thyrotropin releasing hormone receptor)↓, Tacr1(tachykinin receptor 1)↓,*
mmu04724	Glutamatergic synapse	15	*Slc17a7(solute carrier family 17 (sodium-dependent inorganic phosphate cotransporter), member 7)↑, Slc17a6(solute carrier family 17 (sodium-dependent inorganic phosphate cotransporter), member 6)↑, Grm2(glutamate receptor, metabotropic 2)↑, Gls2(glutaminase 2 (liver, mitochondrial))↑, Grm8(glutamate receptor, metabotropic 8)↑, Slc17a8(solute carrier family 17 (sodium-dependent inorganic phosphate cotransporter), member 8)↓ Homer2(homer scaffolding protein 2)↑, Plcb4(phospholipase C, beta 4)↑, Kcnj3(potassium inwardly-rectifying channel, subfamily J, member 3)↑, Dlgap1(discs, large (Drosophila) homolog-associated protein 1)↑, Gng2(guanine nucleotide binding protein (G protein), gamma 2)↑, Adcy1(adenylate cyclase 1)↑, Adcy2(adenylate cyclase 2)↑, Adcy8(adenylate cyclase 8)↑, Gng8(guanine nucleotide binding protein (G protein), gamma 8)↓,*

(*continued on next page*)

Table 2 (*continued*)

KEGG Entry	Term	count	Genes
mmu04725	Cholinergic synapse	14	*Chrna4(cholinergic receptor, nicotinic, alpha polypeptide 4)*↑ *Chrm3(cholinergic receptor, muscarinic 3, cardiac)*↑, *Chrm2(cholinergic receptor, muscarinic 2, cardiac)*↑, *Kcnj6(potassium inwardly-rectifying channel, subfamily J, member 6)*↑, *Kcnj3(potassium inwardly-rectifying channel, subfamily J, member 3)*↑, *Fos(FBJ osteosarcoma oncogene)*↑, *Plcb4(phospholipase C, beta 4)*↑, *Gng2(guanine nucleotide binding protein (G protein), gamma 2)*↑, *Adcy1(adenylate cyclase 1)*↑, *Adcy2(adenylate cyclase 2)*↑, *Adcy8(adenylate cyclase 8)*↑, *Gng8(guanine nucleotide binding protein (G protein), gamma 8)*↓, *Slc5a7(solute carrier family 5 (choline transporter), member 7)*↓, *Chat(choline acetyltransferase)*↓
mmu05032	Morphine addiction	12	*Gabra3(gamma-aminobutyric acid (GABA) A receptor, subunit alpha 3)*↑, *Kcnj3(potassium inwardly-rectifying channel, subfamily J, member 3)*↑, *Gabra1(gamma-aminobutyric acid (GABA) A receptor, subunit alpha 1)*↑, *Kcnj6(potassium inwardly-rectifying channel, subfamily J, member 6)*↑, *Kcnj9(potassium inwardly-rectifying channel, subfamily J, member 9)*↑ *Gng2(guanine nucleotide binding protein (G protein), gamma 2)*↑, *Gabbr2(gamma-aminobutyric acid (GABA) B receptor, 2)*↑, *Adcy1(adenylate cyclase 1)*↑, *Adcy2(adenylate cyclase 2)*↑, *Pde1a(phosphodiesterase 1A, calmodulin-dependent)*↑, *Adcy8(adenylate cyclase 8)*↑, *Gng8(guanine nucleotide binding protein (G protein), gamma 8)*↓
mmu04727	GABAergic synapse	11	*Gabra1(gamma-aminobutyric acid (GABA) A receptor, subunit alpha 1)*↑, *Gls2(glutaminase 2 (liver, mitochondrial))*↑, *Adcy1(adenylate cyclase 1)*↑, *Gabra3(gamma-aminobutyric acid (GABA) A receptor, subunit alpha 3)*↑, *Kcnj6(potassium inwardly-rectifying channel, subfamily J, member 6)*↑, *Gng2(guanine nucleotide binding protein (G protein), gamma 2)*↑, *Adcy2(adenylate cyclase 2)*↑, *Adcy8(adenylate cyclase 8)*↑, *Gabbr2(gamma-aminobutyric acid (GABA) B receptor, 2)*↑, *Gng8(guanine nucleotide binding protein (G protein), gamma 8)*↓, *Hap1(huntingtin associated protein 1)*↓
mmu05033	Nicotine addiction	6	*Chrna4(cholinergic receptor, nicotinic, alpha polypeptide 4)*↑, *Slc17a7(solute carrier family 17 (sodium-dependent inorganic phosphate cotransporter), member 7)*↑, *Slc17a6(solute carrier family 17 (sodium-dependent inorganic phosphate cotransporter), member 6)*↑, *Gabra1(gamma-aminobutyric acid (GABA) A receptor, subunit alpha 1)*↑, *Gabra3(gamma-aminobutyric acid (GABA) A receptor, subunit alpha 3)*↑, *Slc17a8(solute carrier family 17 (sodium-dependent inorganic phosphate cotransporter), member 8)*↓
mmu04721	Synaptic vesicle cycle	7	*Slc17a7(solute carrier family 17 (sodium-dependent inorganic phosphate cotransporter), member 7)*↑, *Slc17a6(solute carrier family 17 (sodium-dependent inorganic phosphate cotransporter), member 6)*↑, *Cplx3(complexin 3)*↑, *Stx1a(syntaxin 1A (brain))*↑, *Slc17a8(solute carrier family 17 (sodium-dependent inorganic phosphate cotransporter), member 8)*↓, *Unc13b(unc-13 homolog B (C. elegans))*↑, *Atp6v0e(ATPase, H + transporting, lysosomal V0 subunit E)*↓
mmu04024	cAMP signaling pathway	13	*Sstr1(somatostatin receptor 1)*↑, *Adcy8(adenylate cyclase 8)*↑, *Adcy1(adenylate cyclase 1)*↑, *Adcy2(adenylate cyclase 2)*↑, *Gabbr2(gamma-aminobutyric acid (GABA) B receptor, 2)*↑, *Chrm2(cholinergic receptor, muscarinic 2, cardiac)*↑, *Ryr2(ryanodine receptor 2, cardiac)*↑, *Sstr2(somatostatin receptor 2))*↑, *Pak1(p21 protein (Cdc42/Rac)-activated kinase 1)*↑, *Bdnf(brain derived neurotrophic factor)*↑, *Fos(FBJ osteosarcoma oncogene)*↑, *Ppp1r1b(protein phosphatase 1, regulatory (inhibitor) subunit 1B)*↓ *Fxyd2(FXYD domain-containing ion transport regulator 2)*↓,
mmu04728	Dopaminergic synapse	10	*Drd3(dopamine receptor D3)*↓, *Kcnj6(potassium inwardly-rectifying channel, subfamily J, member 6)*↑, *Kcnj9(potassium inwardly-rectifying channel, subfamily J, member 9)*↑, *Kcnj3(potassium inwardly-rectifying channel, subfamily J, member 3)*↑, *Fos(FBJ osteosarcoma oncogene)*↑, *Plcb4(phospholipase C, beta 4)*↑, *Gng2(guanine nucleotide binding protein (G protein), gamma 2)*↑, *Mapk11(mitogen-activated protein kinase 11)*↑, *Ppp1r1b(protein phosphatase 1, regulatory (inhibitor) subunit 1B)*↓ *Gng8(guanine nucleotide binding protein (G protein), gamma 8)*↓,
mmu04022	cGMP-PKG signaling pathway	11	*Gucy1a3(guanylate cyclase 1, soluble, alpha 3)*↓ *Slc8a1(solute carrier family 8 (sodium/calcium exchanger), member 1)*↑, *Adra2a(adrenergic receptor, alpha 2a)*↑, *Adcy8(adenylate cyclase 8)*↑, *Mef2c(myocyte enhancer factor 2C)*↑, *Adcy2(adenylate cyclase 2)*↑, *Adcy1(adenylate cyclase 1)*↑, *Plcb4(phospholipase C, beta 4)*↑, *Adra1b(adrenergic receptor, alpha 1b)*↑, *Adra1d(adrenergic receptor, alpha 1d)*↑, *Fxyd2(FXYD domain-containing ion transport regulator 2)*↓,

(*continued on next page*)

Table 2 (*continued*)

KEGG Entry	Term	count	Genes
mmu04360	Axon guidance	9	*Sema7a(sema domain, immunoglobulin domain (Ig), and GPI membrane anchor, (semaphorin) 7A)↑, Rnd1(Rho family GTPase 1)↑, Ntng2(netrin G2)↑, Unc5d(unc-5 netrin receptor D)↑, Pak1(p21 protein (Cdc42/Rac)-activated kinase 1)↑, Robo3(roundabout guidance receptor 3)↑, Ephb3(Eph receptor B3)↑, Ntn1(netrin 1)↓, Epha8(Eph receptor A8)↓,*
mmu04726	Serotonergic synapse	9	*Htr5a(5-hydroxytryptamine (serotonin) receptor 5A)↑, Kcnj6(potassium inwardly-rectifying channel, subfamily J, member 6)↑, Kcnj9(potassium inwardly-rectifying channel, subfamily J, member 9)↑, Kcnj3(potassium inwardly-rectifying channel, subfamily J, member 3)↑, Gng2(guanine nucleotide binding protein (G protein), gamma 2)↑, Ptgs2(prostaglandin-endoperoxide synthase 2)↑, Plcb4(phospholipase C, beta 4)↑, Cyp2d22(cytochrome P450, family 2, subfamily d, polypeptide 22)↓ Gng8(guanine nucleotide binding protein (G protein), gamma 8)↓,*

Note: ↑ indicates up-regulation in the tissue of Nac from Intruder versus control mice, whereas ↓ represents down-regulation.

Table 3
Signaling pathways identified by KEGG based on DEGs data of NAc in Intruder versus Observer.

KEGG Entry	Term	count	Genes
mmu04514	Cell adhesion molecules (CAMs)	6	*Cd99(CD99 antigen)↑, Ncam2(neural cell adhesion molecule 2)↓, Itgb8(integrin beta 8)↓, H2-dmb1(histocompatibility 2, class II, locus Mb1)↑, H2-t22(histocompatibility 2, T region locus 22)↑, H2-t9(histocompatibility 2, T region locus 9)↑,*
mmu04010	MAPK signaling pathway	7	*Fgf11(fibroblast growth factor 11)↑, Hspb1(heat shock protein 1)↑, Map3k6(mitogen-activated protein kinase kinase kinase 6)↑, Ptpn7(protein tyrosine phosphatase, non-receptor type 7)↑, Rps6ka1(ribosomal protein S6 kinase polypeptide 1)↑, Ntrk1(neurotrophic tyrosine kinase, receptor, type 1)↑, Fgf22(fibroblast growth factor 22)↑,*
mmu04725	Cholinergic synapse	3	*Chrm2(cholinergic receptor, muscarinic 2, cardiac)↓, Gng13(guanine nucleotide binding protein (G protein), gamma 13)↑, Creb3l1(cAMP responsive element binding protein 3-like 1)↑,*
mmu04360	Axon guidance	2	*Ntn3(netrin 3)↑, Sema3c(sema domain, immunoglobulin domain (Ig), short basic domain, secreted, (semaphorin) 3C)↓,*
mmu04726	Serotonergic synapse	2	*Htr1d(5-hydroxytryptamine (serotonin) receptor 1D)↑, Gng13(guanine nucleotide binding protein (G protein), gamma 13)↑,*
mmu04728	Dopaminergic synapse	2	*Gng13(guanine nucleotide binding protein (G protein), gamma 13)↑, Creb3l1(cAMP responsive element binding protein 3-like 1)↑,*
mmu04080	Neuroactive ligand-receptor interaction	3	*Htr1d(5-hydroxytryptamine (serotonin) receptor 1D)↑, Rxfp1(relaxin/insulin-like family peptide receptor 1)↓, Chrm2(cholinergic receptor, muscarinic 2, cardiac)↓,*
mmu04020	Calcium signaling pathway	2	*Ryr2(ryanodine receptor 2, cardiac)↓, Chrm2(cholinergic receptor, muscarinic 2, cardiac)↓,*

Note: ↑ indicates up-regulation in the tissue of Nac from Intruder versus control mice, whereas ↓ represents down-regulation.

mice and female CD1 mice was taken out, this C57 intruder mouse was physically attacked by the resident CD1 male mouse that became aggressive due to missing female partner (Fig. 1B). In other words, this intruder C57 mouse experienced physical and psychological stress (PPS) that presumably induced fear memory and anxiety. In the meantime, another C57 mouse was placed in neighboring room of this resident home, in which two rooms were separated by a transparent partition, and viewed this physical attack (Fig. 1B). That is, this C57 observer mouse experienced psychological stress (PS). After experienced these stresses twice a day for five days (Fig. 1A), intruder and observer mice were examined by behavioral tasks to identify their fear memory specific to resident CD1 mouse and anxiety state. Fear memory formation in intruder or observer C57 mice to CD1 mice was judged based on their avoidance to the container including aggressive CD1 resident male mouse as well as less access to the interaction zone at day six (Fig. 2A). Values about the ratio of stay time in the interaction zone with a CD1 or C57 mouse in a small container to stay time in the interaction zone without a CD1 or C57 mouse in this container were measured before and after social stresses for the comparison with their self-control. The significant reductions of ratio of stay time in interaction zone with or without a CD1 aggressor in the small container before and after social defeat and unchange of ratio of stay time in interaction zone with or without a strange C57 mouse in the small container indicate the formation of fear memory specific to CD1 mice in intruder and observer mice (Fig. 2B and C). The test of fear memory formation in C57 mice from three groups is conducted in an social interaction cage that included a container of holding mice, in which a C57 mouse was placed in this container and 30 min after this C57 mice was replaced by CD1 aggressor.

Fig. 2A illustrates the moving traces of control, intruders and

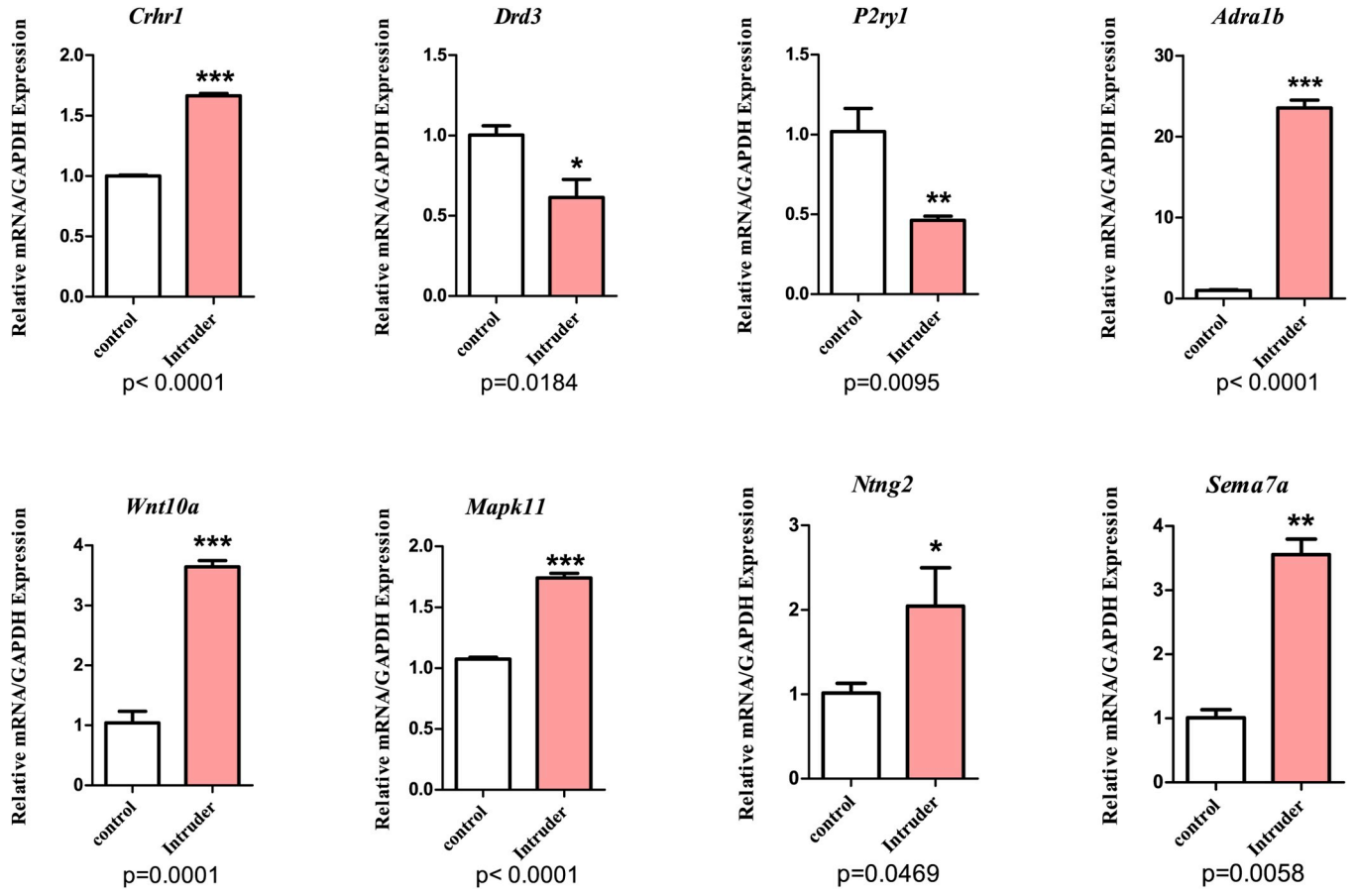

Fig. 4. The validation of differentially expressed mRNAs in the nucleus accumbens from control mice versus Intruder mice. Three asterisks show $p < 0.001$, two asterisks show $p < 0.01$, one asterisk show $p < 0.05$, in which two-sample *t*-test was used for the comparisons between control mice versus Intruder mice.

observers during the social interaction in the absence and presence of CD1 residents at day six. Intruders and observers appear to be fear to CD1 residents. Fig. 2B shows the ratios of stay time in interaction zone from control (blue bar), observer (green) and intruder mice (pink) before (day zero) and after social stress (day six) when a C57 is included in the small container. Fig. 2C shows the ratios of stay time in an interaction zone from intruder, observer and control mice before and after social stress when CD1 aggressor is placed in the small container. Values in intruder mice are 1.25 ± 0.10 before physical/psychological stress and 0.62 ± 0.09 ($p = 0.0002$, $n = 13$, paired *t*-test) after physical/psychological stress. Values in observer mice are 1.18 ± 0.11 before psychological stress and 0.93 ± 0.07 ($p = 0.0399$, $n = 11$, paired-t test) after psychological stress. Values in controls are 1.27 ± 0.10 at day 0 and 1.33 ± 0.17 at day 6 ($p = 0.77$, paired *t*-test, $n = 13$). Compared with no statistical difference among three groups at day 0 ($p = 0.82$, $F = 0.2010$, Total df = 36, one-way ANOVA), there is significant difference among intruder, observer and control mice after the stress ($p < 0.001$, $F = 8.515$, Total df = 36, one-way ANOVA). There is statistical difference in the presence of CD1 versus C57 after the stress (three asterisks, $p < 0.001$; an asterisk, $p < 0.05$; unpaired *t*-test). We analyzed the $Ratio_{CD1}$ results of intruder and observer group on day 6 with two-sample *t*-test ($p = 0.0091$). Fig. 2D shows the number of mice with ratio down (red) or up (gray) from day 0 to day 6 (chi-square test; $p = 0.019$). These data suggest that a mixture of physical and psychological stress or psychological stress only induces fear memory specific to CD1 aggressors, as well as severer fear memory occurs in physical/psychological stress.

Fig. 3A illustrates the moving traces of intruder, observer and control mice on elevated plus maze before (day 0, top panels in 3A) and after social stresses (day 6, bottom panels in 3A). Values of staying in open arms for intruders (red bar), observer (green) and control groups (purple) at day 0 are 9.71 ± 1,45, 9.91 ± 1.97 and 9.72 ± 1.18, respectively (Fig. 3B, $p = 0.995$, $F = 0.004925$, Total df = 36, one-way ANOVA). Values of staying in open arms for intruder (pink), observer (green) and control mice (blue) at day 6 are 3.14 ± 1.21, 4.29 ± 1.90 and 9.01 ± 1.04, respectively (Fig. 3C, $p = 0.0098$, $F = 5.314$, Total df = 36, one-way ANOVA). The data suggest that both physical/psychological stress and psychological stress lead to anxiety.

We subsequently examined molecular mechanisms in the nucleus accumbens underlying fear memory and anxiety in intruder induced by physical/psychological stress and in observer mice induced by psychological stress, in which miRNA and mRNA profiles were analyzed by high throughput sequencing to quantify their expression levels.

3.2. Overall qualities of RNA-Sequencing dataset

With high throughput sequencing, mRNA and miRNA profiles were analyzed in nucleus accumbens tissues from each of mice showing fear memory from intruder group and observer group as well as each of mice from control group ($n = 3$, each group). The selection of these mice for tissue harvests was based on the fact that they express the greatest level of fear memory and anxiety in intruder and observer groups. By filtering reads with low quality and adaptor from RNAs of 53.9–58.37 Mb raw sequence reads (100 bp) in mRNA library Illumina sequencing, 44.3–45.09 Mb clean reads from each library were mapped, i.e., 88.33–93.11% of total reads from mouse genome (UCSC mm10) equivalently for samples (Table S2). Totals about 27,372,899–31,193,770 raw tag counts were produced in small RNA library. After filtering reads with low quality and adaptor, we got clean tag counts in 25,480,795–29,756,564 (Table S3). The distribution of these clean small RNA reads varied in 10–44 nucleotides each library, in

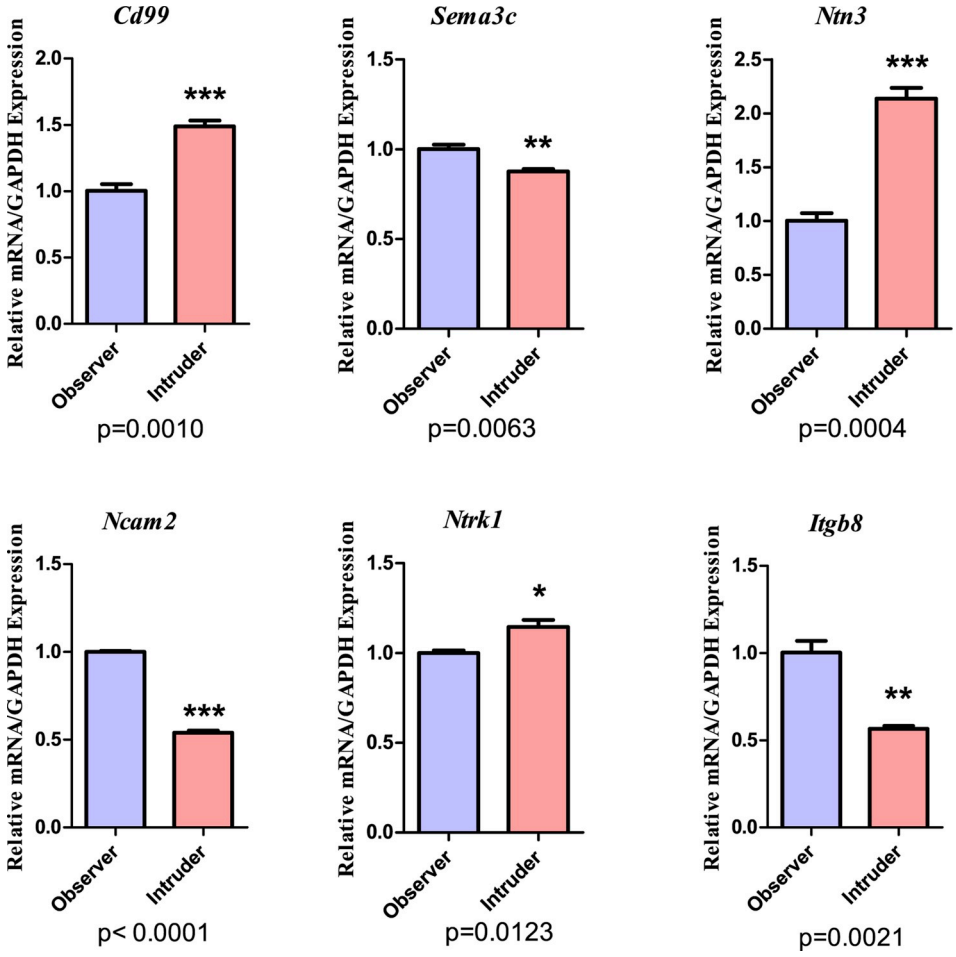

Fig. 5. The validation of differentially expressed mRNAs in the nucleus accumbens from Observer mice versus Intruder mice. Three asterisks show $p < 0.001$, two asterisks show $p < 0.01$, one asterisk show $p < 0.05$, in which two-sample *t*-test was used for the comparisons between control mice versus Intruder mice.

which the most abundant lengths were 22 nucleotides (Fig. S1). High-quality clean reads larger than 18 nucleotides were mapped to mouse genome. Genome-matched reads were divided to different categories of small RNAs based on their biogenesis and annotation (Fig. S2). The most abundant RNA category from each library was miRNA. These transcriptome and small RNA sequencing data with high qualities were used to further analysis.

3.3. mRNA differentiations in the nucleus accumbens among PPS- or PS-induced fear memory versus control mice

mRNAs in the nucleus accumbens were quantified by sequencing total RNAs and their RPKM values were calculated. Except for low expression level (RPKM < 0.5), other genes were analyzed for their differential expression by DESeq2. After mapping reads referred to mouse genome, 17,360 (17,376) mRNAs from clean read sequences with high quality included 8756 (9058) of upregulated mRNAs and 8604 (8318) of downregulated mRNAs while comparing control versus PPS-induced fear memory and control versus PS-induced fear memory. The criterion to confirm the differential expression of genes was the ratio of their RPKM values above 1.5 fold (Biggar and Storey, 2011; Dwivedi et al., 2015; Ma et al., 2016a; Si et al., 2018; Sun et al., 2018). In other words, if the ratio of their RPKM changed above 1.5 folds between control and PPS-induced fear memory, between control and PS-induced fear memory or between PPS-induced fear memory and PS-induced fear memory, the differential expression of mRNAs was warranted.

Taken out those genes in low expression (i.e., the single digit of RPKM values), we found that 552 mRNAs reached the 1.5 fold ratio of PPS-induced fear memory mice to control mice in their RPKM values, in which 242 mRNAs were downregulated and 310 mRNAs were upregulated (Table S4). Table 1 presents these upregulated and downregulated genes related to synapses and signaling pathways in the nucleus accumbens from mice showing PPS-induced fear memory versus control. In synapse-relevant genes, top lines represent those genes of encoding synapse elements and bottom lines show genes that encode signaling pathways of regulating synapses. In genes relevant to signaling pathways, top lines represent genes that encode molecules of constituting signaling pathways and bottom lines show genes that encode molecules of regulating signaling pathway. The upregulated genes related to synapse elements in the nucleus accumbens from PPS-induced fear memory mice include *Adra1b, Adra1d, Adra2a, Chrm3, Grm8, Grm2, Hrh1, Sstr1, Sstr2, Sstr3, Cckbr, Rxfp1, Ntsr1* and *Crhr1*. Based on bioinformatics for mRNA-guided protein translation (KEGG database), these upregulated genes in PPS-induced fear memory mice encode structural proteins of building adrenergic, cholinergic, glutamatergic and histaminergic synapses as well as somatostatin and neurotensin receptors. The downregulated genes related to synapse elements in the nucleus accumbens from PPS-induced fear memory mice include *Drd3, Grik2, Htr2c, Gabrg1, P2ry1, Npy2r, Tacr1* and *Trhr*. According to the analysis of bioinformatics for mRNA-guided protein translation (KEGG database), these downregulated genes in PPS-induced fear memory mice encode structural proteins of building up dopaminergic, glutamatergic, serotonergic, GABAergic and purinergic synapses.

Table 4
The changed miRNAs predict target mRNAs in Intruder versus Control.

miRNAs	The predicted target mRNAs that match DEGs in transcriptome *	miRNAs	The predicted target mRNAs that match DEGs in transcriptome *
miR-483–5p↓	*Tmem178↑, Vwa5b2↑,Cyp26b1↑, Cabyr↑, Wnk4↑, Bdnf↑,Runx2↑, Col24a1↑, Rph3a↑, Lrfn1↑, Cacna1g↑, Lsp1↑ Ptpru↑, Slc5a5↑, Crhr1↑, Hrh1↑, Camk2n1↑, Neurod6↑, Pdlim1↑, Mmgt2↑, Sh2b2↑, Serinc2↑, Cyp26b1↑,*	miR-486a-5p↓	*Efhd2↑, Cacna1g↑, Adgra1↑, Zyx↑, Ntng2↑, Vwa5b2↑, Cyp26b1↑, Igfbp2↑, Rnd1↑, Adra1b↑, Ephb3↑, Hps6↑, Fhod3↑, Relb↑, Cbln2↑, Tgfb1i1↑, Grrp1↑ , Adamtsl2↑, H2-M3↑, Satb2↑,Col26a1↑, Sowahb↑,*
miR-2137↑	*Zcchc12↓, Pcdh17↓, Pds5b↓, Sox1↓, Cbln4↓, Zfp825↓, Plppr1↓,Hscb↓, Dynlt1a↓, Foxp2↓, Cobll1↓, Sncaip↓, Trps1↓, Zfand4↓, Klf8↓, Ranbp17↓, St8sia2↓, Gdnf↓, Gdnf↓, Slitrk6↓,*	miR-375–3p↓	*Nrgn↑, Basp1↑, Tspan17↑, Mical2↑ Klf2↑, Chrm3↑, Grm8↑, Fezf2↑, Gja4↑, Tmem265↑, Bdnf↑, Wnt9a↑, Mroh5↑, Sftpc↑, Serinc2↑, Cacna1g↑, Phospho1↑, Synj2↑, Synj2↑,*
miR-532–5p↓	*Olfm1↑, Lrfn1↑, Cacna1g↑, Slitrk1↑, Cdr2↑, Ak4↑, Cyp26b1↑, Ptpru↑, Adra2a↑, Gls2↑, Adcy8↑, Cd34↑, Hps6↑, Fhod3↑, Cbln1↑, Nr4a2↑, Bdnf↑, Runx2↑, Lsp1↑, Psrc1↑,*	miR-206–3p↓	*Rph3a↑, Ncald↑,1110008P14Rik↑, Phlda3↑, Plekha2↑,Cbln2↑, Bdnf↑, Runx2↑, Col24a1↑, Ly6e↑, C1ql3↑, Slc6a7↑, Synj2↑, Ntsr1↑, Ang↑, Slc5a5↑ , Adcy8↑, Prss23↑,*
miR-490–5p↑	*Caln1↓, Unc13c↓, Dlk1↓, AW551984↓, Ccr5↓, Npy2r↓, Atp6v1c2↓ ,Mttp↓, Myt1↓, Pou2f1↓, Cklf↓, Apol8↓, Gulp1↓, Sfrp1↓, Trps1↓, Zfp85↓, Zfp882↓, Ranbp17↓,*	miR-1247–5p↓	*Sncb↑, Ncald↑, Sulf2↑, Pigyl↑, Slc6a7↑, Zyx↑, Phospho1↑, Synj2↑,Ak4↑, Fhod3↑, Plekha2↑, Nxph3↑, E2f1↑, Adamtsl2↑, Capg↑, Bdnf↑, Galnt15↑, Serinc2↑,*
miR-200b-3p↑	*Gucy1a3↓, Amotl1↓, Kctd8↓, Rapgef6↓, Zdbf2↓, Mttp↓,Ankrd49↓, Mcm5↓, Myt1↓, Ccr5↓, C7↓, Sugct↓, Sncaip↓, Zfand4↓, Zfand4↓, Kif9↓, 1700028K03Rik↓,*	miR-491–5p↓	*Olfm1↑, Sncb↑, Camk2n1↑, Prr18↑, Stx1a↑, Cdk18↑, Psmb10↑, Col11a2↑, Npas1↑, Kcnj6↑, Dkkl1↑, AU021092↑, Bdnf↑, Runx2↑, Cenpm↑, Adgrd1↑,*
miR-200b-5p↑	*Hap1↓, Sesn3↓, Arhgap6↓, Amotl1↓, Cep57↓, A430033K04Rik↓, Rwdd3↓, Sp4↓, N4bp2↓, Dennd4c↓, Clcn5↓, Pcdh11x↓, Gcfc2↓, Ascl1↓, Zfp879↓, Dsg1c↓,*	let-7i-3p↑	*Pde1c↓, Myt1↓, Pcdh11x↓, Ptch2↓, Prss56↓, Mctp1↓, Grik2↓, Cbln4↓, Ska2↓, Pdzd2↓, Zdbf2↓, Foxp2↓, Sp4↓, Rab27b↓, Pik3c2a↓, Pou2f1↓, Pou2f1↓,*
miR-144–3p↑	*Pds5b↓, Arhgap6↓, Cep57↓, Zdbf2↓, Ppat↓, Foxp2↓, Cachd1↓, Lcorl↓, Dhtkd1↓, Myt1↓, Pcdh11x↓, Pou2f1↓, Pou2f1↓, Zc3h12c↓, Cntnap3↓, Klf8↓,*	miR-429–3p↑	*Ufl1↓, Lrrcc1↓, Fndc9↓, Nipal2↓, Cobll1↓, Enox2↓, Ccdc187↓, Dennd4c↓, Atp11c↓, Zc3h12c↓, Gcfc2↓, Cntnap3↓, Zfp882↓, Ranbp17↓, Slitrk6↓,*
miR-3547–3p↓	*Stmn2↑,1110008P14Rik↑, Phlda3↑, Cnih3↑, Lrfn1↑, Vwa5b2↑, Gfra2↑, Mfsd10↑, Sstr1↑, Col11a2↑, Neurod2↑, Akr1e1↑, Wnk4↑, Runx2↑, Cenpm↑,*	miR-3473b↓	*Nptxr↑, Phlda3↑, Limk1↑, Slc6a7↑, Mical2↑, Cacna1g↑, Tnfrsf12a↑, Hps6↑, Fezf2↑, Dhrs11↑, Tgfb1i1↑, Wnt4↑, Adamtsl2↑, Scube1↑, Scube1↑,*
miR-219c-3p↑	*Baiap3↓, Ppp1r2↓, Tshz1↓, Spata13↓, Mttp↓, Man1a↓, Wipf2↓, Bmpr1a↓ , Slc5a7↓, Perp↓, C1qtnf6↓, Nipal2↓, Prrt4↓, Enox2↓, Lca5↓,*	miR-3105–5p↓	*Crhr1↑, Mfsd10↑, Adra2a↑, Adcy8↑, Sel1l3↑, Laptm4b↑, Necab3↑, Plcxd2↑ , Slc5a5↑, Siah3↑, Bdnf↑, Col24a1↑, Neurod2↑, Dhrs11↑,*
miR-133a-3p↓	*Olfm1↑, Laptm4b↑, Ttc9b↑, Slc6a7↑, Lrfn1↑, Synj2↑, Rtn4rl2↑, Lrfn2↑, Hrh1↑, Relb↑, Bdnf↑, Bmp3↑, Slfn2↑, Slc52a3↑,Ephb3↑, Lcn2↑,*	miR-199b-5p↓	*Efhd2↑, Lingo1↑, Adgra1↑, Nptx2↑, Mrm1↑, Nxph3↑, Ccdc3↑, Ifi35↑, Il17ra↑, Scube1↑, 1700016K19Rik↑, Bdnf↑, Galnt15↑, Slc52a3↑,*
miR-489–3p↓	*Mical2↑, Cdr2↑, Nbl1↑, Sstr2↑, Igfbp6↑, Cmbl↑, Adra2a↑, Npas1↑, E2f1↑ , Zbtb46↑, Cabyr↑, Mkx↑, Sowahb↑, Ptges3l↑, Wnt9a↑, Figf↑,*	miR-214–3p↓	*Hapln4↑, Slc36a1↑, Cyp26b1↑, Cyp26b1↑, Ntng2↑, Ntng2↑, Hr↑, Cdh24↑, Nxph3↑, Lsm11↑, Kcns1↑, H2-T9↑, H2-M3↑, Siah3↑, Sh3tc1↑,*
miR-34b-3p↓	*Cbln2↑, Bdnf↑, Col24a1↑, Fblim1↑, Satb2↑, Tspan17↑, Cacna1g↑, Plekho1↑, Nptx2↑, E130012A19Rik↑, Hrh1↑, Tnfrsf12a↑, Krt80↑,*	miR-451a↑	*Baiap3↓, Grik2↓, Grik2↓, Lrrcc1↓, Lrrcc1↓, Khdrbs2↓, Dynlt1a↓, Klf5↓, Fbxo36↓, Ccr5↓, Tex9↓, Pou2f1↓, Trps1↓, Pcdhga1↓,*
miR-6968–3p↓	*Tspan17↑, Lrfn1↑, Nptx1↑, Ccnd1↑, Lrfn2↑, Hs3st2↑, Cd34↑, Zbtb16↑, Neurod2↑, Thpo↑, Bdnf↑, Arhgap25↑,*	miR-141–3p↑	*Ehd4↓, Wnt7a↓, Kctd8↓, Zdbf2↓, Ccdc39↓, Atp6v1c2↓, Pik3c2a↓, Ntn1↓, Nipal2↓, Sp4↓, Rbms3↓, Zbtb26↓, Cntnap3↓, Slitrk6↓,*
miR-199b-3p↓	*Ncald↑, Sulf2↑, Cacna1g↑, Synj2↑, Cdkn1a↑, Ntng2↑, Rnd1↑, Tnfrsf12a↑ , Cpne9↑, Gjc2↑, Zbtb46↑, Kcnk4↑, Runx2↑, Ly6g6e↑,*	miR-341–5p↑	*1110017D15Rik↓, Atp6v1c2↓, Lcorl↓, C7↓, Cd24a↓, Sp4↓, Katnal2↓, Ezh2↓, Prkg1↓, Trps1↓, Wipf2↓, Zkscan16↓, Rps6ka5↓,*
miR-200a-3p↑	*Wfs1↓, Sall1↓, Wipf2↓, Ccdc39↓, Dhtkd1↓, Fam126a↓, Mttp↓, Cc2d2a↓, Fbxo36↓, Lca5↓, Cntnap3↓, Prkg1↓, Fbn1↓,*	miR-192–3p↓	*Nefm↑, Gpx3↑, Tspan17↑, Lrfn1↑, Nrn1↑, Capg↑, Kcnk3↑, Fggy↑, Grm8↑, Lsm11↑, Zbtb46↑, Wnk4↑, Bdnf↑, Arhgap25↑,*
miR-467h↓	*Mkx↑, Hrh1↑, Wnt4↑, Thpo↑, Arhgap15↑, Sulf2↑, Mical2↑,Jdp2↑, Slitrk1↑, Ak4↑, Bdnf↑, Fblim1↑, Fblim1↑,*	miR-670–3p↓	*Ncald↑, Lynx1↑, Limk1↑, Cyp26b1↑, Amn↑, Cdh20↑, Kcnj6↑, Relb↑, Fezf2↑ , Sap30↑, Sox3↑, Tonsl↑, Tuba8↑, Uba7↑, Lsp1↑,*
miR-214–5p↓	*Camk2n1↑, Ier5↑, Sstr1↑, Hrh1↑, Car7↑, Fhod3↑, Sap30↑, E2f1↑, Ybx2↑, Nat8f3↑, Calhm2↑, Mroh5↑, Tmem40↑, Sh3tc1↑,*	miR-1306–5p↓	*Camk2n1↑, Mast1↑, Zdhhc22↑, Synj2↑, Tnfrsf12a↑, Zbtb16↑, Ybx2↑, Gja4↑, Nr4a2↑, Nr4a2↑, Scube1↑, Siah3↑, Runx2↑,*
miR-6965–3p↓	*Gls2↑, Synj2↑, Cyp26b1↑, Necab3↑, Coa4↑, Olfm1↑, Chga↑, Ly6e↑, Sulf2↑, Nrn1↑, Rassf5↑, Nr4a2↑, Tuba8↑, Nmrk1↑,*	miR-5100↓	*Sulf2↑, Sulf2↑, Stac2↑, Rasl11b↑, Nr2c2ap↑, C130074G19Rik↑, Blnk↑, Slfn2↑, Ak4↑, Grm8↑, Klf2↑, Mmgt2↑, Relb↑,*
miR-199a-5p↓	*Ncald↑, Olfm2↑, Limk1↑, Adgra1↑,43352↑, Synj2↑, Ier5↑, Col11a2↑, Hs3st2↑, Klf2↑, Prrg2↑, Slc10a3↑, Nxph3↑,*	miR-499–5p↓	*Nptxr↑, Tmem163↑, Gfra2↑, Sstr2↑, Ier3↑, Col11a2↑, Kcnj6↑, Grm8↑, Nxph3↑, Runx2↑, Lsm11↑, Mroh5↑, Slc52a3↑,*
miR-10b-5p↓	*Shh↑, Cyp26b1↑, Nr2c2ap↑, Tbr1↑, Nxph3↑, Rph3a↑, Ifitm10↑, Mvd↑, Jdp2↑, Synj2↑, Prrg2↑, Ccdc3↑, Arhgap25↑,*	miR-501–5p↓	*Kcnmb4↑, Golga7b↑, Kcnc4↑, Adgra1↑, Jdp2↑, Cd34↑, Neurod6↑, Gadd45a↑, St6galnac4↑, Zbtb46↑, Thpo↑, Lsp1↑,*
miR-202–5p↓	*Cabp1↑, Golga7b↑, Slc36a1↑, Ptpru↑, Mkx↑, Plcxd2↑, Tgfb1i1↑, Il17ra↑, Arhgap15↑, Runx2↑, Nmrk1↑, Rspo3↑,*	miR-199a-3p↓	*Olfm1↑, Ncald↑, Ncald↑, Sulf2↑, Slc6a7↑, Galnt15↑, Serinc2↑, Grm2↑, Prss23↑, Sox3↑, E2f1↑, St6galnac4↑,*
miR-124–3p↑	*Peg10↓, Sall1↓, Bmpr1a↓, Kctd8↓, Rapgef6↓, Pik3c2a↓, Lcorl↓, Pou3f4↓, Atp11c↓, Ccr5↓, Zbtb7c↓, Adam12↓,*	miR-133b-5p↓	*Nrgn↑, Ppdpf↑, Lrfn1↑, Rassf5↑, Kcnj6↑, Sh2b2↑, Tgfb1i1↑, Runx2↑, Sowahb↑, Gpx3↑, Col24a1↑, Arhgap25↑,*
miR-351–5p↓	*Sncb↑, Camk2n1↑, Ncald↑, Nptx1↑, Slc2a6↑, Col11a2↑, Sstr3↑, Kcnq4↑, Eva1b↑, Uba7↑, Col24a1↑,*	miR-10a-5p↓	*Lingo1↑, Nrn1↑, Plekho1↑, Igfbp2↑, Grm2↑, Relb↑, Dkkl1↑, Sstr3↑, E2f1↑, Rspo2↑, Kcnq4↑, Lag3↑, Krt80↑,*
miR-34c-3p↓	*3110035E14Rik↑, Tmem254b↑, Nbl1↑, Plcxd2↑, Adcy8↑, Fhod3↑, Fhod3↑, Scube1↑, Bdnf↑, Slc52a3↑, Sftpc↑,*	miR-200a-5p↑	*Gad2↓, Cirbp↓, Pds5b↓, Arhgap6↓, Wipf2↓, P2ry1↓, Rbms3↓, Dennd4c↓, Pou2f1↓, Svil↓, Cd74↓, Slitrk6↓,*
miR-675–3p↓	*Slc17a7↑, Ncald↑, Ly6e↑, Adra1d↑, Mrm1↑, Ptpn3↑, Prrg2↑, E2f1↑, Tgfb1i1↑, Tle6↑, Arhgap15↑, Psrc1↑,*	miR-135a-1-3p↓	*Rph3a↑, Rph3a↑, Zyx↑, Grm2↑, Cdkn1a↑, Rxfp1↑,Rassf5↑, Adcy8↑, Tnfrsf12a↑, Thpo↑, Chst8↑, Tgfb1i1↑,*
miR-483–3p↓	*Nefm↑, Nefh↑, Cacna1g↑, Tnfrsf12a↑, Chrd↑, Mmgt2↑, Fhod3↑, Amn↑, Gucy2g↑, Wnt9a↑, Cenpm↑, Dmrta2↑,*	miR-3544–3p↓	*Rph3a↑, Nptxr↑, Tmem25↑, Cacna1g↑, Amn↑, Cbln1↑, Nat8f3↑, H2-M3↑, Hrct1↑, Socs3↑, Wnt9a↑, Smoc2↑,*
miR-27a-5p↓	*Stx1a↑, Cdk18↑, Stac2↑, Slitrk1↑, 43352↑, AU021092↑, Tnfrsf12a↑, Crhbp↑, Gadd45a↑, Dgka↑, Capg↑,*	miR-133b-3p↓	*Sema7a↑, Cnih3↑, Slc6a7↑,43352↑, Ak4↑, Neurod2↑, St6galnac4↑, St6galnac4↑, Ngf↑, Rspo3↑, Ang↑,*
miR-297c-5p↑	*Rnpc3↓, Wipf2↓, Amotl1↓, Cachd1↓, Pde1c↓, Pde1c↓, Mob1b↓, Zfp729a↓, Kif9↓, C1qtnf6↓, Slc37a1↓,*	miR-669m-5p↑	*Amotl1↓, Plppr1↓, Rapgef6↓, Rab27b↓, Rbms3↓, Heyl↓, Gpr149↓, Prdm11↓ , Trps1↓, Pou2f1↓, Notum↓,*
miR-208b-3p↓	*Camk2n1↑, Slitrk1↑, Necab3↑, Sstr2↑, Hrh1↑, Lsm11↑, Tmem200a↑, Vip↑, Poc1a↑, Lcn2↑, Col24a1↑,*	miR-3076–5p↓	*Rph3a↑, Nptxr↑, Synj2↑, Cyp26b1↑, Adra2a↑, Chrd↑, Adamtsl2↑, Bco2↑, Bdnf↑, Fblim1↑, Serinc2↑,*
miR-499–3p↓	*Camk2n1↑, Kcnc4↑, Ak4↑, Tnfrsf12a↑, Zbtb16↑, E2f1↑, Scube1↑, Siah3↑ , Bdnf↑, Slc52a3↑,*	miR-103-2-5p↓	*Cabp1↑, Necab3↑, Fggy↑, Fhod3↑, A330050F15Rik↑, H2-T9↑, Capg↑, Ngf↑, Bdnf↑, Cenpm↑, Wnt10a↑,*
miR-5615–3p↓	*Zdhhc22↑, Ak4↑, Mapk11↑, Gls2↑, Cbln2↑, Amn↑, Ccdc3↑, C130074G19Rik↑, Bdnf↑, Uba7↑, Ctla2b↑,*	miR-1a-3p↓	*Stmn2↑, Phlda3↑, Olfm2↑, Nptx1↑, Zyx↑, Mkx↑, Ccnd1↑, Cckbr↑, Scube1↑, Capg↑, Psrc1↑, Satb2↑,*
miR-6945–3p↓	*Gjc2↑, Stx1a↑, Zyx↑, St8sia5↑, Slc36a1↑, Ak4↑, Klf2↑, Cbln2↑, Tonsl↑, Eva1b↑, Stab1↑, Lsp1↑,*	miR-7213–5p↑	*Cartpt↓, Spata13↓, Slc5a7↓, Pdzd2↓, Plce1↓, C1qtnf6↓, 1110017D15Rik↓, Slc37a1↓, Thsd7a↓,*

(*continued on next page*)

Table 4 (*continued*)

miRNAs	The predicted target mRNAs that match DEGs in transcriptome *	miRNAs	The predicted target mRNAs that match DEGs in transcriptome *
miR-3074–5p↑	*Rsph1↓, Rnpc3↓, Cox6b2↓, Ccdc187↓, N4bp2↓, Swt1↓, Plce1↓, Mfap2↓, Trps1↓, Kif9↓, Adam12↓,*	miR-675–5p↓	*Laptm4b↑, Slc2a6↑, Cdkn1a↑, Rasl10a↑, Ybx2↑, Capg↑, Thpo↑, Bdnf↑, Runx2↑, Dmrta2↑, Hr↑,*
miR-540–5p↑	*Gad2↓, Sv2c↓, AW551984↓, Arhgap6↓, Rfc4↓, Gm14391↓, N4bp2↓, Plce1↓, S100a3↓, Prss56↓,*	miR-7019–3p↑	*Gucy1a3↓, Spata13↓, Amotl1↓, Zdbf2↓, Stk26↓, Adamts20↓, Prss56↓, Atp6v1c2↓, Rbms3↓,*
miR-344e-5p↓	*Olfm1↑, Sulf2↑, Sulf2↑, Grm2↑, Igfbp6↑, Shh↑, Rspo2↑, Runx2↑, Lsp1↑, Lcn2↑, Cdkn1a↑,*	miR-669f-5p↑	*Ccdc166↓, Etohi1↓, Fndc9↓, Adamts3↓, Sp4↓, Rfc4↓, Hmgcs2↓, Tex9↓, Sfrp1↓, S100a3↓,*
miR-669p-5p↓	*Bok↑, Galnt9↑, Igfbp2↑, Ak4↑, Col11a2↑, Adra1b↑, Lypd6b↑, Tmem40↑,*	miR-879–5p↑	*Adamts3↓, Pde1c↓, Mob1b↓, Pou3f4↓, Clcn5↓, Pou2f1↓, Fam179a↓,*
miR-34c-5p↓	*Cck↑, Phospho1↑, Slitrk1↑, Plcxd2↑, Gls2↑, Cebpb↑, Lsm11↑, Sstr3↑, Cabyr↑, Syna↑,*	miR-3106–5p↑	*Grik2↓, Slc37a1↓, Cutc↓, Zbtb26↓, Atp11c↓, Trps1↓, Gdnf↓, 1700028K03Rik↓,*
miR-341–3p↑	*Pcdh17↓, Rapgef6↓, Rab27b↓, Rab27b↓, Dhtkd1↓, Ptch2↓, Pou2f1↓, Pou2f1↓,*	miR-6538↑	*Zkscan16↓, Amotl1↓,1110017D15Rik↓, Erich3↓, Cobll1↓, Notum↓, Lama5↓,*
miR-466d-5p↓	*Zdhhc22↑, Slc5a5↑, Ephb3↑, Fhod3↑, Siah3↑, Eva1b↑, Fblim1↑,*	miR-7008–5p↑	*Gad2↓, Col6a1↓, Ehd4↓, Wipf2↓, Slc37a1↓, Ntn1↓, Ccno↓,*

Note: ↑ indicates up-regulation in the tissue of Nac from Intruder versus control mice, whereas ↓ represents down-regulation.

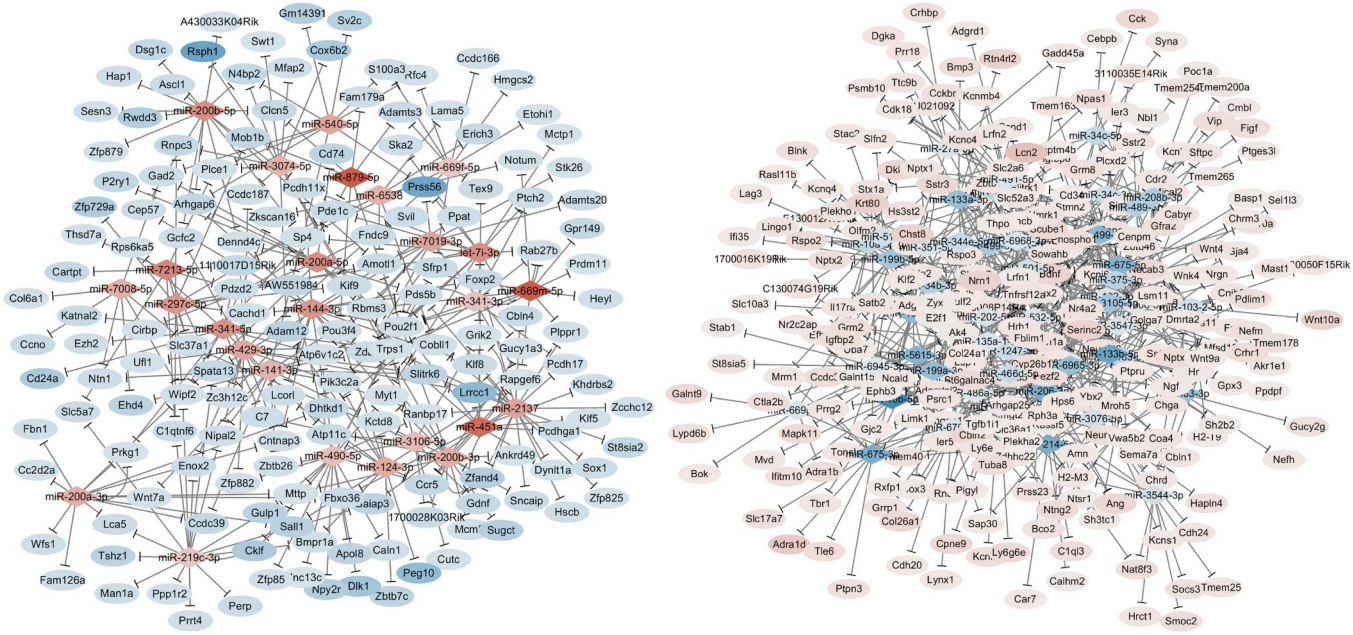

Fig. 6. MicroRNA-mRNA network in control mice versus Intruder mice. microRNA/mRNA networks were constructed between the 78 miRNAs and 411 overlapped mRNAs with using transcriptome expression data and predicted target genes from RNAhybrid, Targetscan and miRanda databases. Red symbols present the elevated expression of miRNAs or mRNAs and the deeper the red, the more upregulated. Blue symbols present the down regulated miRNAs or mRNAs and the deeper the blue, the more downregulated. (For interpretation of the references to colour in this figure legend, the reader is referred to the Web version of this article.)

In terms of the signaling pathways that regulate synapse functions, the downregulated genes in the nucleus accumbens in PPS-induced fear memory mice include *Gucy1a3, Prkg1, Pde1c, Plce1, Wnt7a* and *Fzd4*. Based on bioinformatics for mRNA-guided protein translation (KEGG database), these downregulated genes in PPS-induced fear memory mice encode cGMP, cAMP, calcium and Wnt signaling pathways. On the other hand, the upregulated genes include *Cacna1g, Wnt4, Wnt10a, Fzd9, Bdnf, Ngf, Ntng2, Mapk11* and *Adcy8,* i.e., the involvement of calcium, Wnt, MAPK, cAMP and axon guidance signaling pathways. It is noteworthy that certain genes of encoding synapse elements appear upregulated and some genes of regulating these synapses appear downregulated in the nucleus accumbens from PPS-induced fear memory mice, indicating the imbalance in the regulation of synaptic functions. In addition to an imbalance among genes in a signaling pathway, the upregulated and downregulated multiple signaling pathways make entire molecular networks in the nucleus accumbens be imbalance, which lead to neural dysfunction. In summary, the upregulated genes of encoding synapse elements may strengthen the formation and transmission of synapses for fear memory (Wang and Cui, 2018). The imbalance of signaling pathways may be involved in elevated anxiety mood and fear memory induced by physical/psychological stress.

Furthermore, our study showed that 658 mRNAs had the 1.5 fold ratio of PS-induced fear memory mice to control mice in RPKM values, in which 387 mRNAs are downregulated and 271 mRNAs are upregulated (Table S6). The involved synapses and signaling pathways in the nucleus accumbens are listed in Table 2. The upregulated genes in relevance to synapse elements include *Adra1b, Adra1d, Adra2a, Chrm2, Chrm3, Chrna4, Gabra1, Gabbr2, Gabra3, Grm2, Grm8, Htr5a, Hrh1, Sstr1, Sstr2, Sstr3, Cckbr, Nmbr, Rxfp1, Ntsr1, Crhr1*. Based on bioinformatics for mRNA-guided protein translation (KEGG database), the upregulated genes in PS-induced fear memory mice encode the structural elements of adrenergic, cholinergic, GABAergic, glutaminergic, serotonergic, histaminergic and neuropeptide synapses. The downregulated genes related to synapse elements in the nucleus accumbens from PS-induced fear memory mice include *Drd3, P2ry1, Npy2r, Tacr1, Trhr* and *Lpar6*. Based on bioinformatics for mRNA-guided protein translation (KEGG database), these downregulated genes in PS-induced fear memory mice encode structural proteins of building dopaminergic, purinergic and neuropeptide synapses.

In terms of signaling pathways, the downregulated genes in the nucleus accumbens include *Gng8, Gucy1a3, Chat, Fxyd2, Ppp1r1b, Tacr1, Trhr* and *Cyp2d22*. Based on the bioinformatics for mRNA-guided protein translation (KEGG database), the downregulated genes in PS-

Table 5
The changed miRNAs predict target mRNAs in Intruder versus Observer.

miRNAs	The predicted target mRNAs that match DEGs in transcriptome *	miRNAs	The predicted target mRNAs that match DEGs in transcriptome *
miR-669p-5p↓	*Tmem256↑, Ifi27↑, Ifi27↑, Crocc↑, Tnnt1↑, Tmem53↑, Zbtb20↑, Oscar↑, Nme6↑, Nmb↑, Idua↑,*	miR-375–3p↓	*1700030K09Rik↑, Sh2d5↑, Alkbh7↑, Nrtn↑, Csf2ra↑, Tmem53↑, Olfr287↑, Pear1↑, Rab42↑,*
let-7a-1-3p↓	*Ppp1r14a↑, Metrn↑, Rps6ka1↑, Trh↑, Ldb3↑, Dmkn↑, Fam179a↑, Aurka↑, Ptpn7↑,*	miR-34b-5p↓	*Lynx1↑, Coa4↑, Nme6↑, H2-T22↑, Ntn3↑, Capg↑, Oscar↑, Lcn2↑, Ggnbp1↑,*
miR-200b-3p↑	*Arl5b↓, Lysmd3↓, Ccr5↓, Sugct↓, Fgd4↓, Plcxd3↓, Adm↓, Sntb2↓, Xkr7↓,*	miR-141–3p↑	*Kcnk9↓, Nvl↓, Ccdc39↓, Zfp654↓, Vasn↓, Cep85l↓, Pcdh18↓, Sntb2↓,*
miR-101a-5p↑	*Mbd5↓, Ryr2↓, Bach1↓, Plch1↓, Clcn5↓, Mgat4c↓, 2210404O09Rik↓,*	miR-541–3p↑	*Hecw1↓, Bach1↓, Plch1↓, Syt10↓, Arl5b↓, Tmem74↓, Nqo1↓, Cdh12↓,*
miR-200c-3p↑	*Cbln4↓, Slc19a2↓, Lcorl↓, Palm2↓, Hecw1↓, Kctd16↓,*	miR-466c-3p↑	*Slc16a1↓, Cbln4↓, Insc↓, Palm2↓, Rbks↓, Nt5c1a↓, Kctd16↓,*
miR-200a-3p↑	*Ccdc39↓, Slc19a2↓, Hecw1↓, Tmem74↓, Plcxd3↓, Pcdha4↓,*	miR-96–5p↑	*Ccdc39↓, Plch1↓, Mob1b↓, Syt10↓, Kctd16↓, Tmem202↓,*
miR-540–5p↑	*Cyb5d1↓, Plch1↓, Rfc4↓, Gm14391↓, Lysmd3↓, Sntb2↓,*	miR-135a-1-3p↓	*Syndig1l↑, Ifi27↑, Ifi27↑, Kif17↑, Pear1↑, Ptpn7↑,*
miR-34c-3p↓	*Fau↑, Josd2↑, Lgals3bp↑, Tmem53↑, Ifit3b↑, Ptpn7↑,*	miR-3105–5p↓	*Nmb↑, Dhrs11↑, Zbtb20↑, Ndst2↑, Hck↑, Pld6↑,*
miR-182–5p↑	*0610010B08Rik↓, Mbd5↓, Gm14391↓, Syt10↓,*	miR-341–5p↑	*Xylt1↓, Lcorl↓, Fgd4↓, Sntb2↓, Serpinb8↓,*
miR-6240↓	*Fggy↑, Pcdhga2↑, Pear1↑, Rab42↑,*	miR-34c-5p↓	*Ppp1r14a↑, Tpd52l1↑, Rps6ka1↑, Oscar↑,*
miR-124–3p↑	*Kcnk9↓, Chrm2↓, Lcorl↓, Ccr5↓, Zfp366↓,*	miR-377–5p↑	*Chrm2↓, Ccr5↓, Sugct↓, 2210404O09Rik↓,*
miR-341–3p↑	*Bicd1↓, Bicd1↓, Dok6↓, Tenm1↓, Sntb2↓,*	miR-467h↓	*Fgf11↑, Setd6↑, Krt10↑, Idua↑, Idua↑,*
miR-3473e↓	*Tusc1↑, Dhrs11↑, Cd164l2↑, Dmrta2↑,*	miR-200b-5p↑	*Pgm2l1↓, Hecw1↓, Clcn5↓, Tmem202↓,*
miR-34b-3p↓	*Ntrk1↑, Fam221b↑, Itga2b↑, Mutyh↑,*	miR-879–5p↑	*Mid1↓, Mob1b↓, Clcn5↓, Fgd4↓,*
miR-673–5p↑	*Rbks↓, Ccr5↓, Fgd4↓, Utp14b↓,*	miR-7662–3p↑	*Chdh↓, Vasn↓, Adm↓, Pcdh18↓,*
miR-33–5p↑	*Pcdh18↓, Mgat4c↓, Serpinb8↓,*	let-7i-3p↑	*Cbln4↓, Plcxd3↓, Pcdhgb5↓,*
miR-551b-3p↑	*Mbd5↓, Plch1↓, Serpinb8↓,*	miR-544–3p↑	*Ncam2↓, Med11↓, Zfp366↓,*
miR-3065–5p↑	*Arsk↓, Pcdha10↓, Pcdha4↓,*	miR-193a-3p↑	*Nvl↓, Slc19a2↓, Chrdl1↓,*
miR-206–3p↑	*Lcorl↓, Plch1↓, Chrdl1↓,*	miR-3074–5p↑	*Cox6b2↓, Swt1↓, Sntb2↓,*
miR-199b-3p↑	*Ccdc39↓, Fgd4↓, Cdh12↓,*	miR-212–5p↑	*Slc19a2↓, Plch1↓,*
miR-144–3p↓	*Crocc↑, Spint1↑,*	miR-7019–3p↑	*Ncam2↓, Mid1↓,*
miR-532–3p↑	*Kcnk9↓, Xkr7↓,*	miR-3106–5p↑	*Chdh↓,*
miR-188–5p↑	*Xylt1↓,*	miR-5100↓	*Ntn3↑,*
miR-203–5p↑	*Rxfp1↓,*		

Note: ↑ indicates up-regulation in the tissue of Nac from Intruder versus control mice, whereas ↓ represents down-regulation.

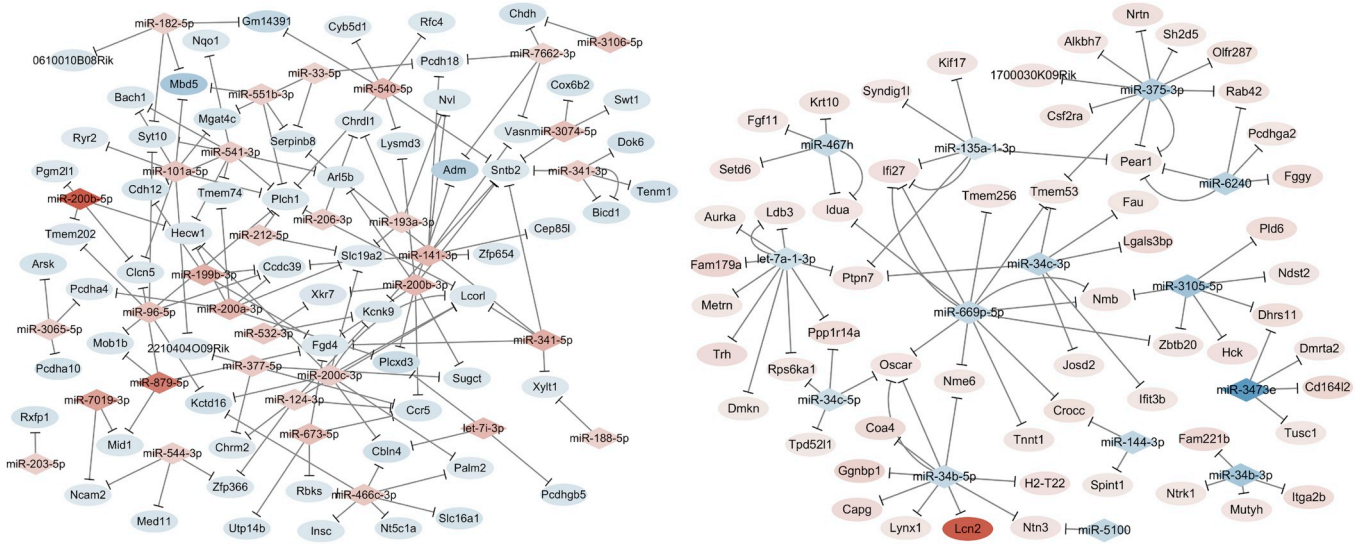

Fig. 7. MicroRNA-mRNA network in Observer mice versus Intruder mice. microRNA/mRNA networks were constructed between the 47 miRNAs and 122 overlapped mRNAs with using transcriptome expression data and predicted target genes from RNAhybrid, Targetscan, and miRanda databases. Red symbols present the elevated expression of miRNAs or mRNAs and the deeper the red, the more upregulated. Blue symbols present the down regulated miRNAs or mRNAs and the deeper the blue, the more downregulated. (For interpretation of the references to colour in this figure legend, the reader is referred to the Web version of this article.)

induced fear memory mice encode signaling pathways for cGMP, cAMP, phosphatase and P450. One the other hand, the upregulated genes include *Adcy1, Adcy2, Adcy8, Pde1a, Plcb4, Ryr2, Gng2, Pak1m Mapk11, Napepld, Bdnf, Ntng2* and *Rnd1*. Based on bioinformatics for mRNA-guided protein translation (KEGG database), the upregulated genes in PS-induced fear memory mice encode the signaling pathways for cAMP, calcium, protein kinase, phosphatase and axon guidance. In these data, some genes of encoding signaling pathways are upregulated and some genes of regulating these signaling pathways are downregulated from PS-induced fear memory, indicating the imbalance in each of signaling pathways. In addition to the imbalance among genes in a single signaling pathway, the upregulated and downregulated multiple signaling pathways make entire molecular networks in the nucleus accumbens be imbalance, which may lead to neuronal dysfunction. Thus, the upregulated genes of encoding signaling pathways that regulate synapse elements may strengthen the formation and transmission of synapses for fear memory (Wang and Cui, 2018). The imbalanced status of signaling pathways may be involved in elevated anxiety mood and fear memory induced by psychological stress.

It is noteworthy that some genes encoding synapse elements and signal pathways in the nucleus accumbens from PPS- and PS-induced fear memory are overlap (Tables 1~2). The upregulation of *Adra1b, Adra1d, Adra2a, Chrm3, Grm8, Grm2* and *Adcy8* as well as the downregulation of *Drd3, P2ry1, Npy2r* and *Gucy1a3* in both PPS- and PS-

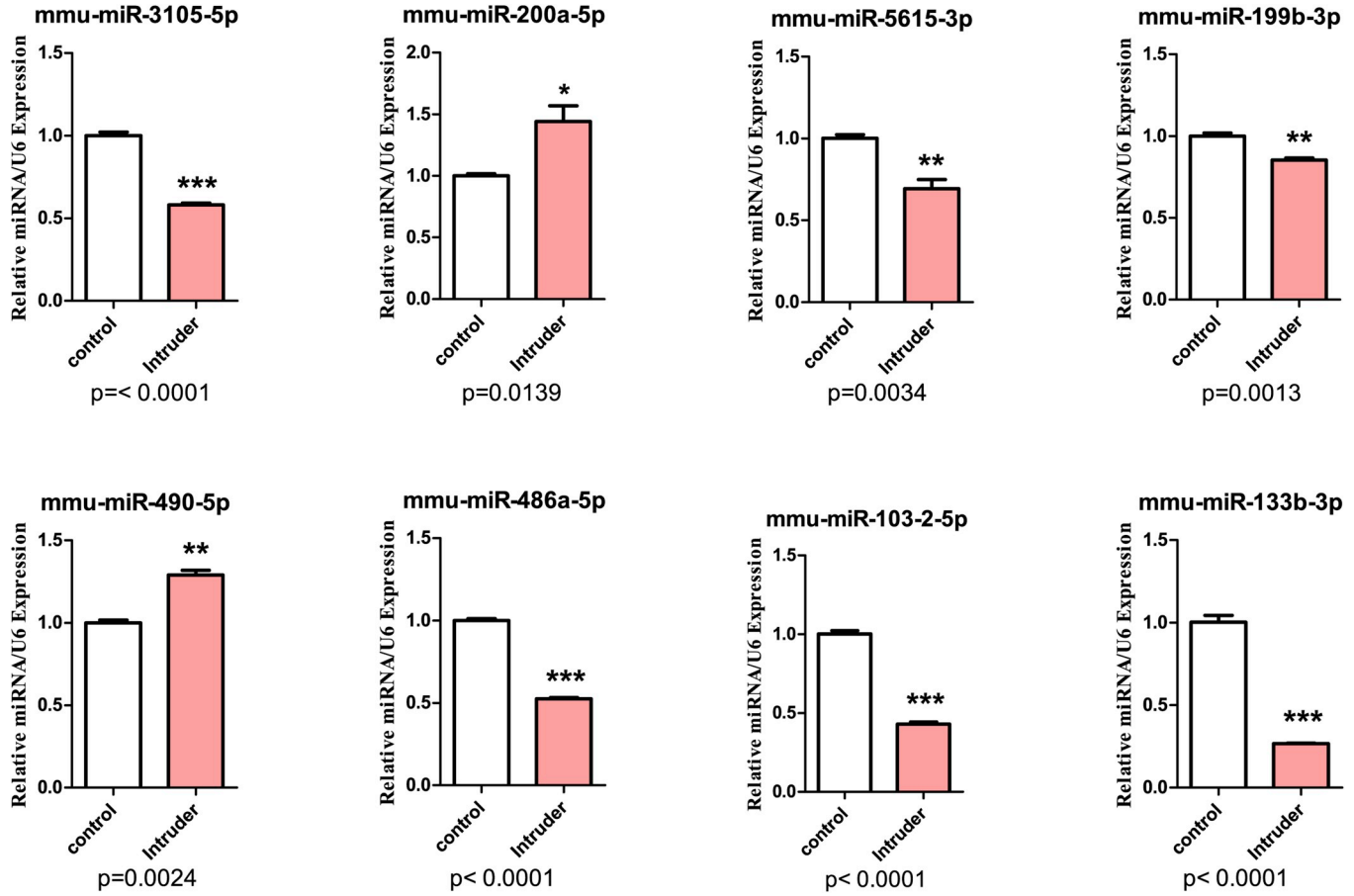

Fig. 8. The validation of differentially expressed microRNAs in nucleus accumbens from control mice versus Intruder mice. Three asterisks show $p < 0.001$, two asterisks show $p < 0.01$, one asterisk show $p < 0.05$, in which two-sample *t*-test was used for the comparisons between control mice versus Intruder mice.

induced fear memory indicate that these genes are relevant to the psychological stress. Table 3 presents the differential expressions of certain genes from intruders with PPS-induced fear memory versus observers with PS-induced fear memory. Since Tables 1∼2 present the differential expression of genes from fear memory of intruder mice versus controls or fear memory of observer mice versus controls, the upregulated or downregulated expression of those genes in Table 3 for intruders versus observers indicates real differences in the two groups. In fear memory from observer mice versus intruder mice, *Cd99, Fgf11, Ntrk1, Gng13, Creb3l1, Ntn3 and Htr1d* are upregulated, whereas *Ncam2, Itgb8, Chrm2, Sema3c, Rxfp1 and Ryr2* are downregulated. That is, the differential expressions of these genes in the nucleus accumbens for different outcomes between PPS-induced fear memory and PS-induced fear memory are located in neural pathways of cholinergic, serotonergic, glutamatergic and GABAergic synapses as well as signaling pathways of calcium and cell adhesion molecules.

To validate our data above, we ran quantitative RT-PCR (qRT-PCR) from nucleus accumbens tissues that had been used for mRNA sequencing. The expressions of *Drd3* and *P2ry1* are lowered as well as the expressions of *Crhr1*, *Adra1b*, *Wnt10a*, *Mapk11*, *Ntng2* and *Sema7a* are elevated in PPS-induced fear memory mice, compared to control mice (Fig. 4). The expressions of *Sema3c, Ncam2* and *Itgb8* are lowered, as well as the expressions of *Cd99, Ntn3* and *Ntrk1* are elevated in PPS-induced fear memory mice, compared with PS-induced fear memory mice (Fig. 5). These consistent results achieved by mRNA sequencing and qRT-PCR analysis validate our study.

Based on the interaction between mRNAs and miRNAs, the expression of mRNAs in cells is influenced by miRNAs, through which the bindings of miRNAs with their dicers degrade mRNAs and weaken their translations (Afonso-Grunz and Muller, 2015; Beilharz et al., 2010; Dalmay, 2013; Valinezhad Orang et al., 2014). If the downregulation of mRNAs in the nucleus accumbens for fear memory and anxiety is caused by miRNAs, their correspondent miRNAs are upregulated, or vice versa. To validate mRNA changes in our study, we quantitatively analyzed miRNA profiles by their sequencings in nucleus accumbens tissues from the mice with PPS-induced fear memory in intruder mice, PS-induced fear memory in observer mice and control mice.

3.4. miRNA expressions in the nucleus accumbens among PPS- or PS-induced fear memory versus control mice

The profile of miRNAs is given in Table S9 if their expressions change above 2 folds in intruder mice with PPS-induced fear memory versus control mice, in which certain miRNAs are upregulated or downregulated. Their predicted target mRNAs match measures from mRNA sequencing data above based on the databases (RNAhybrid, Targetscan and miRanda) about interactions between miRNAs and mRNAs. Table 4 presents the altered miRNAs and their predicted-target mRNAs from intruder mice and control mice. Table S13 presents the altered mRNAs and their correspondent miRNAs from intruder mice and control mice. The interactive networks about miRNAs and overlapped mRNAs for intruder mice and control mice, which were based on transcriptome expression data and predicted target genes from three databases, were made in the Cytoscape (Fig. 6). By reading Tables S10, 4 and S13, we can find that the regulation of mRNAs and the regulation of miRNAs are matched well.

The profile of miRNAs is demonstrated in Table S11 if their expressions change above 2.0 folds in intruder mice with PPS-induced fear memory versus observer mice with PS-induced fear memory, in which some miRNAs are upregulated or downregulated. The predicted

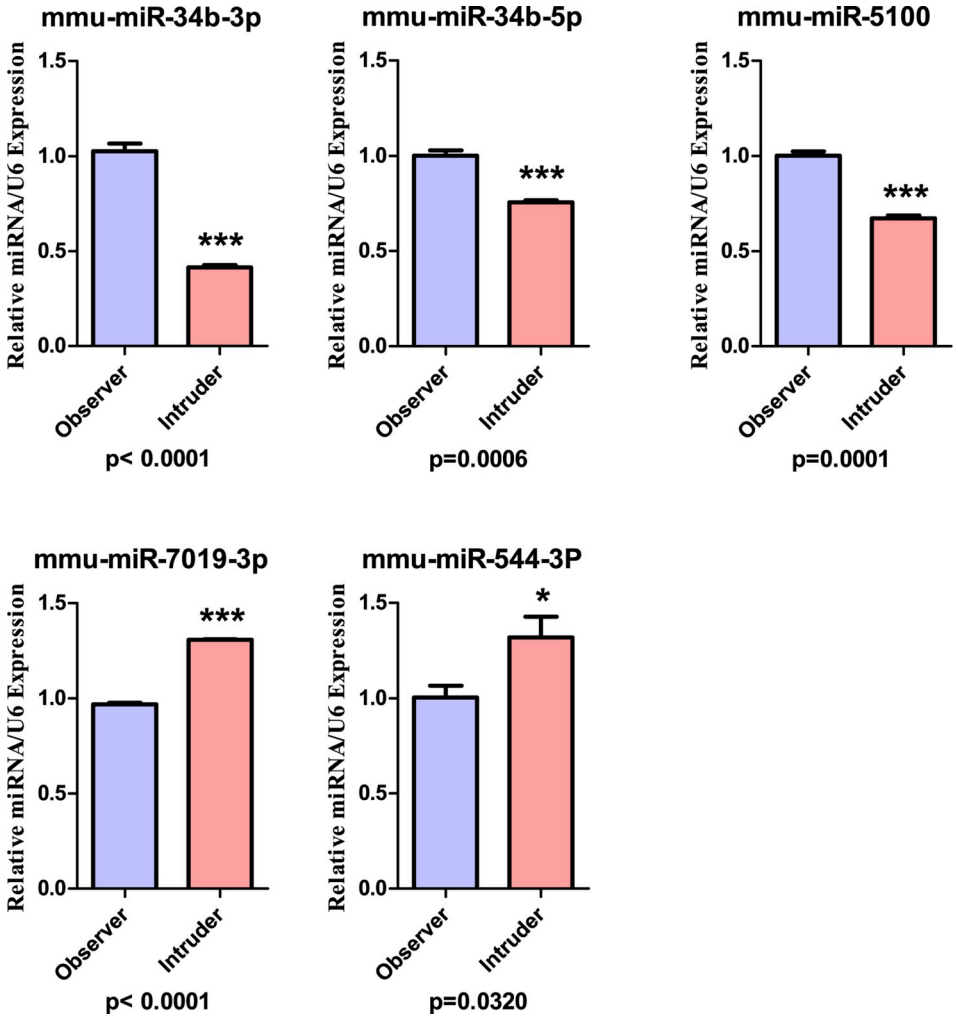

Fig. 9. The validation of differentially expressed microRNAs in nucleus accumbens from Observer mice versus Intruder mice. Three asterisks show $p < 0.001$, two asterisks show $p < 0.01$, one asterisk show $p < 0.05$, in which two-sample *t*-test was used for the comparisons between control mice versus Intruder mice.

target mRNAs match measures by mRNA sequencing data based on RNAhybrid, Targetscan and miRanda about interaction between miRNAs and mRNAs. Table 5 shows the altered miRNAs and their predicted-target mRNAs from intruder mice versus observer mice. Table S14 shows the altered mRNAs and their correspondent miRNAs from intruder versus observer mice. Interactive networks about miRNAs and overlapped mRNAs for intruders versus observers, which were based on transcriptome data and predicted target genes from three databases, were made in the Cytoscape (Fig. 7). By reading Tables S12, 5 and S14, we can see that the regulation of mRNAs and the regulation of miRNAs are matched well. Consistent results by jointly sequencing mRNAs and miRNAs validate our analyses and strengthen our conclusion.

In order to validate data by sequencing miRNA analysis, we selected certain miRNAs to conduct qRT-PCR, including miR-3105–5p, miR-200a-5p, miR-5615–3p, miR-199b-3p, miR-490–5p miR-486a-5p, miR-103-2-5p and miR-133b-3p in intruder mice with PPS-induced fear memory versus control mice (Fig. 8) as well as miR-34b-5p, miR-34b-3p, miR-5100, miR-7019–3p and miR-544–3p in intruder mice versus observer mice (Fig. 9). Consistent to data by high-throughput sequencing, these miRNAs are significantly changed in qRT-PCR analysis from intruder mice with PPS-induced fear memory versus control mice (Fig. 8) as well as intruder mice versus observer mice (Fig. 9). Their predicted target mRNAs match the actually altered mRNAs (Tables 4~5, S10, S12~S14). Consistent results from analyses by miRNA sequencing and qRT-PCR analysis support the validation of our study. It is pointed out that some miRNAs reversely express in intruder mice with PPS-induced fear memory versus observer mice with PS-induced fear memory (Fig. 9). In other words, these miRNAs may influence mice with fear memory induced physical/psychological stress (Table S11).

3.5. Crhr1 and Adra1b mRNA are the targets of miRNA-483–5p and miRNA-699p-5p, respectively

To validate the silico prediction in Tables 4~5, we examined whether miRNA-483–5p and miRNA-699p-5p targeted to *Crhr1* and *Adra1b*, respectively, by qRT-PCR and dual luciferase reporter assay. The inverse correlations are seen between *Crhr1* and miRNA-483–5p (Fig. 10A) as well as between *Adra1b* and miRNA-699p-5p (Fig. 10C) from qRT-PCR analyses. In the dual luciferase report assay, we constructed luciferase reporter plasmids, which contained the wild-type or the mutant of the predicted binding sites of miRNAs in mRNAs *Crhr1* and *Adra1b*. Such reporter constructs were transfected into HEK293T cells. The relative activities of luciferase reporter for mRNAs *Crhr1* and *Adra1b* are significantly attenuated by the mimics of miRNA-483–5p and miRNA-699p-5p, respectively, but not negative control (Fig. 10B/10D). These attenuations are reversed by mutating the binding sites of miRNA-483–5p and miRNA-699p-5p in *Crhr1* and *Adra1b*, respectively. These results support that mRNA *Crhr1* is a direct target of miRNA-483–5p and mRNA *Adra1b* is a direct target of miRNA-699p-5p, which are consistent with our bioinformatics analyses in the prediction of miRNA target genes.

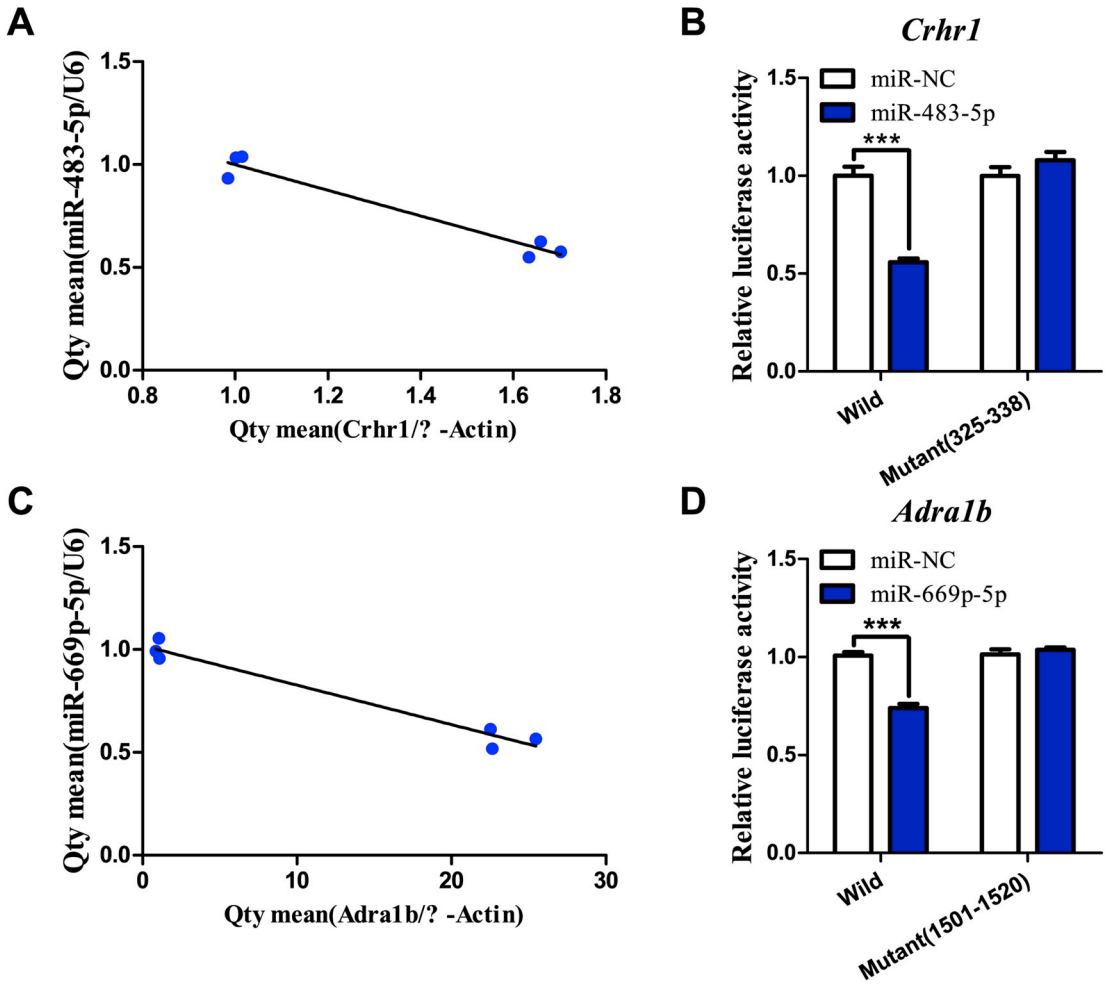

Fig. 10. The miRNAs targeted mRNAs were validated by qRT-PCR and Luciferase reporter assay. A) The correlation between miR-483–5p and its prediction target *Crhr1* expression by qRT-PCR in nucleus accumbens tissue (r = −0.9493; p = 0.001). **B)** Luciferase reporter assay performed by constructed luciferase reporter plasmids, which contained the wild-type or the mutant of the predicted binding sites of miR-483–5p in *Crhr1*. Then co-transfection of wild or mutant type vectors with miR-483–5p mimic or negative control (NC) into HEK293T cells. (P = 0.0009, two-sample *t*-test). **C)** The correlation between miR-669p-5p and its prediction target *Adra1b* expression by qRT-PCR in nucleus accumbens tissue(r = −0.9619; p = 0.0006). **D)** Luciferase reporter assay performed by constructed luciferase reporter plasmids, which contained the wild-type or the mutant of the predicted binding sites of miR-669p-5p in *Adra1b*. Then co-transfection of wild or mutant type vectors with miR-669p-5p mimic or negative control (NC) into HEK293T cells.(P = 0.0006, two-sample *t*-test).

4. Discussion

By high throughput sequencings of mRNAs and miRNAs, we have quantitatively analyzed their changes in nucleus accumbens tissues from intruder mice with PPS-induced fear memory, observer mice with PS-induced fear memory and control mice. In intruder mice of expressing PPS-induced fear memory and anxiety versus controls, the upregulated mRNAs relevant to synapses include *Adra1b, Adra1d, Adra2a, Chrm3, Grm8, Grm2, Hrh1, Sstr1, Sstr2, Sstr3, Cckbr, Rxfp1, Ntsr1* and *Crhr1*, whose encoded proteins build up adrenergic, cholinergic, glutamatergic and histaminergic synapses as well as somatostatin and neurotensin receptors. These results indicate that the functions of adrenergic, cholinergic, glutamatergic and histaminergic synapses are enhanced in fear memory and anxiety induced by physical and psychological stress. On the other hand, the downregulated genes are *Drd3, Grik2, Htr2c, Gabrg1, P2ry1, Npy2r, Tacr1* and *Trhr*, which encode proteins for dopaminergic, glutamatergic, serotonergic, GABAergic and purinergic synapses. These results indicate that the functions of dopaminergic, serotonergic, GABAergic and purinergic synapses are weakened in fear memory and anxiety induced by physical/psychological stress. In terms of signaling pathways that regulate synapse function, the downregulated genes include *Gucy1a3, Prkg1, Pde1c, Plce1, Wnt7a* and *Fzd4*, which encode cGMP, cAMP, calcium and Wnt signaling pathways. The upregulated genes include *Cacna1g, Wnt4, Wnt9a, Fzd9, Bdnf, Ngf, Ntng2, Mapk11* and *Adcy8,* which encode calcium, Wnt, MAPK, cAMP and axon guidance signaling pathways. The upregulation or downregulation of the genes included in cAMP, calcium and Wnt signals indicates the incoordination of molecules consisting of such signaling pathways in fear memory and anxiety induced by physical and psychological stress.

In observer mice of expressing PS-induced fear memory and anxiety versus controls, the upregulated genes relevant to synapse elements include *Adra1b, Adra1d, Adra2a, Chrm2, Chrm3, Chrna4, Gabra1, Gabbr2, Gabra3, Grm2, Grm8, Htr5a, Hrh1, Sstr1, Sstr2, Sstr3, Cckbr, Nmbr, Rxfp1, Ntsr1, Crhr1*, which encode structural elements of adrenergic, cholinergic, GABAergic, glutaminergic, serotonergic, histaminergic and neuropeptide synapses. The results indicate that the functions of adrenergic, cholinergic, GABAergic, glutaminergic, serotonergic, histaminergic synapses are strengthened during fear memory and anxiety induced by psychological stress. On the other hand, those downregulated genes include *Drd3, P2ry1, Npy2r, Tacr1, Trhr* and *Lpar6*, which encode structures of dopaminergic, purinergic and neuropeptide synapses. The data indicate that the functions of dopaminergic and purinergic synapses are weakened during fear

memory and anxiety induced by psychological stress. In terms of signaling pathways, the downregulated genes are *Gng8, Chat, Gucy1a3, Fxyd2, Ppp1r1b, Tacr1, Trhr* and *Cyp2d22,* which encode cGMP, cAMP, phosphatase and P450 signaling pathways. The upregulated genes are *Adcy1, Adcy2, Adcy8, Pde1a, Plcb4, Ryr2, Gng2, Pak1m Mapk11, Bdnf, Napepld, Ntng2* and *Rnd1*, which encode signaling pathways for cAMP, calcium, protein kinase, phosphatase and axon guidance. The upregulation or downregulation of the genes of encoding cAMP and protein kinase pathways indicates the incoordination of molecules consisting of these signaling pathways in fear memory and anxiety induced by physical and psychological stress.

In the comparisons between intruders and observers, the upregulation of *Adra1b, Adra1d, Adra2a, Chrm3, Grm8, Grm2* and *Adcy8* as well as the downregulation of *Drd3, P2ry1, Npy2r* and *Gucy1a3* are observed in both PPS- and PS-induced fear memory. The overlapped alternations in the expression of certain genes for both groups of intruders and observers may be commonly functional to psychological stress and anxiety. These synapses include adrenergic, cholinergic, glutamatergic and dopaminergic synapses. On the other hand, some genes show differential changes. For instance, *Chrna4, Chrm2, Gabra1, Adcy1, Adcy2, Gabbr2, Gabra3, Pak1m, Pde1a, Plcb4, Ryr2 and Gng2* are upregulated, whereas *Grik2, Htr2c, Gabrg1, Gng8, Gng13, Chat, Creb3l1, Map3k6, Ntrk1, Ppp1r1b and Fxyd2* are downregulated. Different outcomes between intruders with PPS-induced fear memory and observers with PS-induced fear memory may result from the differential expressions of some genes that encode those elements of cholinergic, glutamatergic and GABAergic synapses as well as the signaling pathways of cAMP and protein kinases. These results indicate that the imbalanced upregulation and downregulation of genes that encode element molecules for some synapses and signaling pathways may make synapses and neurons in the nucleus accumbens be vulnerable to physical/psychological stress and psychological stresses for suffering from fear memory and anxiety.

Stressful social activities often induce fear memory (Baldi and Bucherelli, 2015; Izquierdo et al., 2016; Makkar et al., 2010). Stress types include physical stress versus psychological stress as well as acute severe stress versus chronic mild stress (Liu et al., 2014; Ma et al., 2016b; Si et al., 2018; Sun et al., 2018; Wang and Lu, 2018). Stress-induced fear memory can drive emotion reactions toward anxiety or depression, and even secondary disorders (Coutellier and Usdin, 2011; Desmedt et al., 2015; Orsini and Maren, 2012; Parsons and Ressler, 2013). The erasing of fear memory is expected to diminish the pathological emotions (de Quervain et al., 2017; Flores et al., 2018; Maren, 2011; Sandkuhler and Lee, 2013). The elucidation of comprehensive molecular profiles for fear memory and memories to negative events by different types of stresses is needed for developing therapeutic targets for releasing these affective disorders (Ma et al., 2016b; Sutoo and Akiyama, 2002; Xu et al., 2015). In the present study, we focus on analyzing mRNA and miRNA profiles in the nucleus accumbens from the mice treated by physical stress and/or psychological stress. In comparison with the electrical stimulus to induce fear memory in previous studies, the social stress induced by physical and/or psychological injuries is more close to the life (Martinez et al., 1998; Tsankova et al., 2006; Vasconcelos et al., 2015).

The level of anxiety and fear memory in response to CD1 resident aggressor appears dominant in intruders versus observers (Fig. 2∼3). To this outcome, the physical/psychological stress based on associative signals from the visual system and the somatosensory system in intruders may be stronger than psychological stress based on the signal only from the visual cortex in observers (Wang, J.-H., 2019; Wang and Lu, 2018). Primary associative memory cells recruited in visual and somatosensory cortices and their convergent innervations onto secondary associative memory cells in the nucleus accumbens of the intruders would be more active than associative memory cells in the nucleus accumbens of the observers (Wang and Cui, 2017, 2018). In terms of molecular mechanisms, these behavioral and cellular changes may be caused by the differential expression levels of some common genes (Tables 1∼2) and/or the difference of certain genes (Tables 1–3). For instance, the expression of genes *Adra1b, Adra1d, Adra2a, Chrm3, Grm8, Grm2* and *Adcy8* is elevated approximately 30% higher in intruders than observers. *Chrna4, Chrm2, Gabra1, Gabbr2, Adcy1, Gabra3, Adcy2, Pde1a, Plcb4, Ryr2, Gng2* and *Pak1m* are upregulated, while *Grik2, Htr2c, Gabrg1, Gng8, Gng13, Chat, Creb3l1, Map3k6, Ntrk1, Fxyd2* and *Ppp1r1b* are downregulated in intruders, in comparison to observers. In other words, the different functional changes in adrenergic, cholinergic, glutamatergic, dopaminergic and GABAergic synapses as well as in the signaling pathways of cAMP and protein kinases may be the reasons for differences in the strength of fear memory and anxiety induced by physical/psychological stress and psychological stress only.

In addition to the downregulation or upregulation of all genes in some signaling pathways, the imbalanced expression of genes in other signaling pathways may play role in fear memory and anxiety induced by psychological stress alone and physical/psychological stress. As indicated in Tables 1–3, some genes in given signaling pathways are elevated in their expressions, while others in these pathways are lowered in the nucleus accumbens from mice with PPS-induced fear memory, indicating the imbalance of molecular networks relevant to synapse elements and signaling pathways. The imbalanced expression among some genes in single signaling pathway may be responsible for PPS-induced fear memory and anxiety, whereas less bidirectional alternations of these genes in intra-signaling pathways may occur in PS-induced fear memory and anxiety. The upregulation and downregulation among multiple signaling pathways as well as among the genes in intra-signaling pathways make molecular networks in the nucleus accumbens to be imbalance, which lead to neuronal and synaptic dysfunctions in the nucleus accumbens for stress-induced fear memory and anxiety.

Genes and their translated proteins are presumably relevant to psychological stress in social defeat and fear memory if their expressions alter in the same direction in fear memory and anxiety induced by psychological stress alone and physical/psychological stress, compared with control. This hypothesis is based on the fact that both groups of mice receive psychological stress, but strengths in their fear memory and anxiety are distinct. Through comparing mRNAs among control, PPS-induced fear memory and PS-induced fear memory about the separated and overlapped changes, we can see that certain genes are specifically changed for PPS-induced fear memory or for PS-induced fear memory (Fig. 4∼5). These results help us to figure out the genes related to psychological stress and fear memory. Genes changed in the same direction in the nucleus accumbens from intruders and observers are likely involved in psychological stress-induced fear memory.

Relationships between stress-induced fear memory and synapses/signaling pathways are explained below. The elevated expression of genes whose encoding proteins build adrenergic, cholinergic and glutamatergic synapses as well as the low expression of genes that encode dopaminergic and purinergic synapses in the nucleus accumbens from intruders and observers indicate that the functional changes in these synapses are responsible for PPS- and PS-induced fear memory. In the meantime, genes that encode intracellular cAMP and phospholipase C are elevated in the nucleus accumbens from intruders and observers, which may upregulate the molecules in adrenergic, cholinergic and glutamatergic synapses. In other words, consistent changes in synapses and signaling pathways constitute the foundation for fear memory and anxiety induced by physical/psychological stress. Furthermore, the upregulated and downregulated changes of genes that encode synapses and signaling pathways lead to the imbalance and instability of molecular networks that may make the vulnerability of neurons and synapses for neural disorders.

In terms of the validation of our study and result, we have done the high throughput sequencing of mRNAs and miRNAs, the quantitative RT-PCR of some RNAs as well as the analysis of interactions between mRNAs and mRNA. Our results indicate that the changed expression of

mRNAs matches the changed expression of miRNAs in high throughput sequencing (Tables 4~5, S13 and S14). Some genes with their altered expressions in high throughput sequencing have been confirmed by qRT-PCR analysis (Fig. 3~4 and 8~9). Furthermore, direct interactions between mRNA *Crhr1* and miRNA-483–5p as well as between *Adra1b* and miRNA-699p-5p are confirmed by dual luciferase report analysis (Fig. 10). Taken these analyses together, we are confident to our results, which is better than previous analyses in either miRNAs or mRNAs.

In addition to our study, molecular mechanisms for depression induced by social defeat has been analyzed by RNA sequencing in the prefrontal cortex, amygdala, nucleus accumbens and ventral hippocampus (Bagot et al., 2016). In this study, an integrative network biology approach has been used to identify transcriptional networks and key driver genes that regulate susceptibility to depressive-like symptoms. Some novel transcriptional networks in relevance to controlling stress susceptibility are identified in the prefrontal cortex, amygdala, nucleus accumbens and ventral hippocampus, which is advanced to study molecular profile in multiple brain areas up to date. Our result in some molecules of the nucleus accumbens is similar to Bagot's study, though others are not. This difference may be due to the uses of different approaches to the analysis of RNA, such as mRNA plus microRNA sequencing in our study and RNA sequencing in Bagot's study. The difference may also result from non-identical paradigm to be used, such as social defeat with physical and psychological stress for five days in our study and social defeat for ten days in Bagot's study. With the combined analyses of mRNA and microRNA sequencing and the consistent result, our data indicate a chain reaction from social stress, microRNA expressional changes that regulate mRNA transcription in the nucleus accumbens to fear memory. The data from both studies should shad light onto revealing the molecular mechanisms underlying social stress and its relevant affective disorders.

We have focused on analyzing and comparing mRNA and miRNA profiles in the nucleus accumbens from intruders with PPS-induced fear memory and observers with PS-induced fear memory, which helps figuring out the molecules that are involved in fear memory and anxiety. The nucleus accumbens is presumably involved in emotion reaction to stress. If fear memory is due to social stress, the analysis of molecular profiles in the nucleus accumbens from PPS-induced and PS-induced fear memory mice should help to figure out the role of the nucleus accumbens in fear memory and anxiety based on molecules analyzed. The alternations of certain genes have not been observed in previous analyses (Cestari et al., 2014; Johansen et al., 2011; Kyrke-Smith and Williams, 2018; Otis et al., 2015), such as molecules related to basic elements of adrenergic, glutamatergic, cholinergic, dopaminergic and serotonergic synapses as well as signaling pathways for intracellular cAMP and calcium. These genes in the nucleus accumbens may be newly working for fear memory and anxiety. Finally, if molecules are commonly changed in PPS-induced fear memory and PS-induced fear memory, they will be targets for developing therapeutic strategies.

It remains to be addressed about the cellular architecture underlying fear memory and anxiety induced by physiological and psychological stresses. As fear memory induced by social defeat is associative in physical attacks and CD1 residents, in which somatosensory cortices and the visual cortex are coactivated, associative memory cells (Wang et al., 2013, 2015) may be recruited. Based on the distribution and working principle of associative memory cells (Wang, J.-H., 2019; Wang and Lu, 2018; Wang and Cui, 2017), we assume that primary associative memory cells are recruited in the visual and somatosensory cortices, and that their convergent synapse innervations onto secondary associative memory cells in the nucleus accumbens of the intruders and observers (Sun et al., 2019; Wang, J.H., 2019a). In addition, secondary associative memory cells are likely recruited in the prefrontal cortex, the hippocampus and the amygdala (Sun et al., 2019; Wang et al., 2018, 2019).

Authors contributions

K Du, W Lu and Y Sun contributed to experiments and data analyses. Jin-Hui Wang contributed to concept, project design and paper writing.

Conflicts of interest

All authors declare no competing interest. All authors have read and approved the final version of the manuscript.

Conflicts of interest

All authors declare no competing interest. All authors have read and approved the final version of the manuscript.

Acknowledgement

This study is funded by National Key R&D Program of China (2016YFC1307101) and Natural Science Foundation of China (81671071 and 81471123) to JHW.

Appendix A. Supplementary data

Supplementary data to this article can be found online at https://doi.org/10.1016/j.jpsychires.2019.08.013.

References

Afonso-Grunz, F., Muller, S., 2015. Principles of miRNA-mRNA interactions: beyond sequence complementarity. Cell. Mol. Life Sci. 72 (16), 3127–3141.
Anderson, E.M., Larson, E.B., Guzman, D., Wissman, A.M., Neve, R.L., Nestler, E.J., Self, D.W., 2018. Overexpression of the histone dimethyltransferase G9a in nucleus accumbens shell increases cocaine self-administration, stress-induced reinstatement, and anxiety. J. Neurosci. 38 (4), 803–813.
Bagot, R.C., Cates, H.M., Purushothaman, I., Lorsch, Z.S., Walker, D.M., Wang, J., Huang, X., Schluter, O.M., Maze, I., Pena, C.J., Heller, E.A., Issler, O., Wang, M., Song, W.M., Stein, J.L., Liu, X., Doyle, M.A., Scobie, K.N., Sun, H.S., Neve, R.L., Geschwind, D., Dong, Y., Shen, L., Zhang, B., Nestler, E.J., 2016. Circuit-wide transcriptional profiling reveals brain region-specific gene networks regulating depression susceptibility. Neuron 90 (5), 969–983.
Baldi, E., Bucherelli, C., 2015. Brain sites involved in fear memory reconsolidation and extinction of rodents. Neurosci. Biobehav. Rev. 53, 160–190.
Barrot, M., Wallace, D.L., Bolanos, C.A., Graham, D.L., Perrotti, L.I., Neve, R.L., Chambliss, H., Yin, J.C., Nestler, E.J., 2005. Regulation of anxiety and initiation of sexual behavior by CREB in the nucleus accumbens. Proc. Natl. Acad. Sci. U.S.A. 102 (23), 8357–8362.
Beilharz, T.H., Humphreys, D.T., Preiss, T., 2010. miRNA Effects on mRNA closed-loop formation during translation initiation. Prog. Mol. Subcell. Biol. 50, 99–112.
Berton, O., McClung, C.A., Dileone, R.J., Krishnan, V., Renthal, W., Russo, S.J., Graham, D., Tsankova, N.M., Bolanos, C.A., Rios, M., Monteggia, L.M., Self, D.W., Nestler, E.J., 2006. Essential role of BDNF in the mesolimbic dopamine pathway in social defeat stress. Science 311 (5762), 864–868.
Biggar, K.K., Storey, K.B., 2011. The emerging roles of microRNAs in the molecular responses of metabolic rate depression. J. Mol. Cell Biol. 3 (3), 167–175.
Bjorkqvist, K., 2001. Social defeat as a stressor in humans. Physiol. Behav. 73 (3), 435–442.
Blanchard, R.J., McKittrick, C.R., Blanchard, D.C., 2001. Animal models of social stress: effects on behavior and brain neurochemical systems. Physiol. Behav. 73 (3), 261–271.
Bosch-Bouju, M., Larrieu, T., Linders, L., Manzoni, O.J., Laye, S., 2016. Endocannabinoid-Mediated plasticity in nucleus accumbens controls vulnerability to anxiety after social defeat stress. Cell Rep. 16 (5), 1237–1242.
Cestari, V., Rossi-Arnaud, C., Saraulli, D., Costanzi, M., 2014. The MAP(K) of fear: from memory consolidation to memory extinction. Brain Res. Bull. 105, 8–16.
Coutellier, L., Usdin, T.B., 2011. Enhanced long-term fear memory and increased anxiety and depression-like behavior after exposure to an aversive event in mice lacking TIP39 signaling. Behav. Brain Res. 222 (1), 265–269.
Dalmay, T., 2013. Mechanism of miRNA-mediated repression of mRNA translation. Essays Biochem. 54, 29–38.
de Quervain, D., Schwabe, L., Roozendaal, B., 2017. Stress, glucocorticoids and memory: implications for treating fear-related disorders. Nat. Rev. Neurosci. 18 (1), 7–19.
Desmedt, A., Marighetto, A., Piazza, P.V., 2015. Abnormal fear memory as a model for posttraumatic stress disorder. Biol. Psychiatry 78 (5), 290–297.
Dwivedi, Y., Roy, B., Lugli, G., Rizavi, H., Zhang, H., Smalheiser, N.R., 2015. Chronic corticosterone-mediated dysregulation of microRNA network in prefrontal cortex of rats: relevance to depression pathophysiology. Transl. Psychiatry 5, e682.
Ehrlich, I., Humeau, Y., Grenier, F., Ciocchi, S., Herry, C., Luthi, A., 2009. Amygdala

inhibitory circuits and the control of fear memory. Neuron 62, 757–771.
Fadok, J.P., Darvas, M., Dickerson, T.M.K., Palmiter, R.D., 2010. Long-term memory for pavlovian fear conditioning requires dopamine in the nucleus accumbens and basolateral amygdala. PLoS One 5 (9).
Fanselow, M.S., Gale, G.D., 2003. The amygdala, fear, and memory. Ann. N. Y. Acad. Sci. 985, 125–134.
Feng, J., Pena, C.J., Purushothaman, I., Engmann, O., Walker, D., Brown, A.N., Issler, O., Doyle, M., Harrigan, E., Mouzon, E., Vialou, V., Shen, L., Dawlaty, M.M., Jaenisch, R., Nestler, E.J., 2017. Tet1 in nucleus accumbens opposes depression- and anxiety-like behaviors. Neuropsychopharmacology 42 (8), 1657–1669.
Flores, A., Fullana, M.A., Soriano-Mas, C., Andero, R., 2018. Lost in translation: how to upgrade fear memory research. Mol. Psychiatry 23, 2122–2132. https://doi.org/10.1038/s41380-017-0006-0.
Floresco, S.B., 2015. The nucleus accumbens: an interface between cognition, emotion, and action. Annu. Rev. Psychol. 66, 25–52.
Francis, T.C., Lobo, M.K., 2017. Emerging role for nucleus accumbens medium spiny neuron subtypes in depression. Biol. Psychiatry 81 (8), 645–653.
Friedlander, M.R., Lizano, E., Houben, A.J., Bezdan, D., Banez-Coronel, M., Kudla, G., Mateu-Huertas, E., Kagerbauer, B., Gonzalez, J., Chen, K.C., LeProust, E.M., Marti, E., Estivill, X., 2014. Evidence for the biogenesis of more than 1,000 novel human microRNAs. Genome Biol. 15 (4), R57.
Friedlander, M.R., Mackowiak, S.D., Li, N., Chen, W., Rajewsky, N., 2012. miRDeep2 accurately identifies known and hundreds of novel microRNA genes in seven animal clades. Nucleic Acids Res. 40 (1), 37–52.
Fu, K.Q., Miyamoto, Y., Sumi, K., Saika, E., Muramatsu, S., Uno, K., Nitta, A., 2017. Overexpression of transmembrane protein 168 in the mouse nucleus accumbens induces anxiety and sensorimotor gating deficit. PLoS One 12 (12).
Ganzel, B.L., Morris, P.A., Wethington, E., 2010. Allostasis and the human brain: integrating models of stress from the social and life sciences. Psychol. Rev. 117 (1), 134–174.
Garrett, A., Chang, K., 2008. The role of the amygdala in bipolar disorder development. Dev. Psychopathol. 20 (4), 1285–1296.
Golden, S.A., Covington 3rd, H.E., Berton, O., Russo, S.J., 2011. A standardized protocol for repeated social defeat stress in mice. Nat. Protoc. 6 (8), 1183–1191.
Goyens, J., Noirot, E., 1975. Effects of cohabitation with females on aggressive behavior between male mice. Dev. Psychobiol. 8 (1), 79–84.
Hammels, C., Pishva, E., De Vry, J., van den Hove, D.L., Prickaerts, J., van Winkel, R., Selten, J.P., Lesch, K.P., Daskalakis, N.P., Steinbusch, H.W., van Os, J., Kenis, G., Rutten, B.P., 2015. Defeat stress in rodents: from behavior to molecules. Neurosci. Biobehav. Rev. 59, 111–140.
Haruno, M., Kimura, M., Frith, C.D., 2014. Activity in the nucleus accumbens and amygdala underlies individual differences in prosocial and individualistic economic choices. J. Cogn. Neurosci. 26 (8), 1861–1870.
Hastings, R.S., Parsey, R.V., Oquendo, M.A., Arango, V., Mann, J.J., 2004. Volumetric analysis of the prefrontal cortex, amygdala, and hippocampus in major depression. Neuropsychopharmacology 29 (5), 952–959.
He, J., Chen, Q., Wei, Y., Jiang, F., Yang, M., Hao, S., Guo, X., Chen, D., Kang, L., 2016. MicroRNA-276 promotes egg-hatching synchrony by up-regulating brm in locusts. Proc. Natl. Acad. Sci. U. S. A. 113 (3), 584–589.
Herry, C., Johansen, J.P., 2014. Encoding of fear learning and memory in distributed neuronal circuits. Nat. Neurosci. 17 (12), 1644–1654.
Heshmati, M., Golden, S.A., Pfau, M.L., Christoffel, D.J., Seeley, E.L., Cahill, M.E., Khibnik, L.A., Russo, S.J., 2016. Mefloquine in the nucleus accumbens promotes social avoidance and anxiety-like behavior in mice. Neuropharmacology 101, 351–357.
Hikida, T., Morita, M., Macpherson, T., 2016. Neural mechanisms of the nucleus accumbens circuit in reward and aversive learning. Neurosci. Res. 108, 1–5.
Ikemoto, S., 2007. Dopamine reward circuitry: two projection systems from the ventral midbrain to the nucleus accumbens-olfactory tubercle complex. Brain Res. Rev. 56 (1), 27–78.
Izquierdo, I., Furini, C.R., Myskiw, J.C., 2016. Fear memory. Physiol. Rev. 96 (2), 695–750.
Johansen, J.P., Cain, C.K., Ostroff, L.E., LeDoux, J.E., 2011. Molecular mechanisms of fear learning and memory. Cell 147 (3), 509–524.
Keele, N.B., 2005. The role of serotonin in impulsive and aggressive behaviors associated with epilepsy-like neuronal hyperexcitability in the amygdala. Epilepsy Behav. 7 (3), 325–335.
Kim, K.S., Lee, K.W., Baek, I.S., Lim, C.M., Krishnan, V., Lee, J.K., Nestler, E.J., Han, P.L., 2008. Adenylyl cyclase-5 activity in the nucleus accumbens regulates anxiety-related behavior. J. Neurochem. 107 (1), 105–115.
Kochenborger, L., Zanatta, D., Berretta, L.M., Lopes, A.P.F., Wunderlich, B.L., Januario, A.C., Neto, J.M., Terenzi, M.G., Paschoalini, M.A., Faria, M.S., 2012. Modulation of fear/anxiety responses, but not food intake, following alpha-adrenoceptor agonist microinjections in the nucleus accumbens shell of free-feeding rats. Neuropharmacology 62 (1), 427–435.
Kyrke-Smith, M., Williams, J.M., 2018. Bridging synaptic and epigenetic maintenance mechanisms of the engram. Front. Mol. Neurosci. 11, 369.
Lebow, M.A., Chen, A., 2016. Overshadowed by the amygdala: the bed nucleus of the stria terminalis emerges as key to psychiatric disorders. Mol. Psychiatry 21 (4), 450–463.
Lee, J.H., Lee, S., Kim, J.H., 2017. Amygdala circuits for fear memory: a key role for dopamine regulation. The Neuroscientist 23 (5), 542–553.
Levita, L., Hoskin, R., Champi, S., 2012. Avoidance of harm and anxiety: a role for the nucleus accumbens. Neuroimage 62 (1), 189–198.
Lim, B.K., Huang, K.W., Grueter, B.A., Rothwell, P.E., Malenka, R.C., 2012. Anhedonia requires MC4R-mediated synaptic adaptations in nucleus accumbens. Nature 487 (7406), 183–189.
Liu, B., Feng, J., Wang, J.-H., 2014. Protein kinase C is essential for kainate-induced anxiety-related behavior and glutamatergic synapse upregulation in prelimbic cortex. CNS Neurosci. Ther. 20 (in press).
Livak, K.J., Schmittgen, T.D., 2001. Analysis of relative gene expression data using real-time quantitative PCR and the 2(-Delta C(T)) Method. Methods 25 (4), 402–408.
Ma, K., Guo, L., Xu, A., Cui, S., Wang, J.H., 2016a. Molecular mechanism for stress-induced depression assessed by sequencing miRNA and mRNA in medial prefrontal cortex. PLoS One 11 (7), e0159093.
Ma, K., Xu, A., Cui, S., Sun, M., Xue, Y., Wang, J.-H., 2016b. Impaired GABA synthesis, uptake and release are associated with depression-like behaviors induced by chronic mild stress. Transl. Psychiatry 6 (e910), 1–10.
Makkar, S.R., Zhang, S.Q., Cranney, J., 2010. Behavioral and neural analysis of GABA in the acquisition, consolidation, reconsolidation, and extinction of fear memory. Neuropsychopharmacology 35 (8), 1625–1652.
Maren, S., 2011. Seeking a spotless mind: extinction, deconsolidation, and erasure of fear memory. Neuron 70 (5), 830–845.
Martinez, M., Calvo-Torrent, A., Pico-Alfonso, M.A., 1998. Social defeat and subordination as models of social stress in laboratory rodents: a review. Aggress. Behav. 24, 241–256.
Meerlo, P., Sgoifo, A., Turek, F.W., 2002. The effects of social defeat and other stressors on the expression of circadian rhythms. Stress 5 (1), 15–22.
Monk, C.S., Klein, R.G., Telzer, E.H., Schroth, E.A., Mannuzza, S., Moulton 3rd, J.L., Guardino, M., Masten, C.L., McClure-Tone, E.B., Fromm, S., Blair, R.J., Pine, D.S., Ernst, M., 2008. Amygdala and nucleus accumbens activation to emotional facial expressions in children and adolescents at risk for major depression. Am. J. Psychiatry 165 (1), 90–98.
Montagud-Romero, S., Blanco-Gandia, M.C., Reguilon, M.D., Ferrer-Perez, C., Ballestin, R., Minarro, J., Rodriguez-Arias, M., 2018. Social defeat stress: mechanisms underlying the increase in rewarding effects of drugs of abuse. Eur. J. Neurosci. 48 (9), 2948–2970.
Orsini, C.A., Maren, S., 2012. Neural and cellular mechanisms of fear and extinction memory formation. Neurosci. Biobehav. Rev. 36 (7), 1773–1802.
Otis, J.M., Werner, C.T., Mueller, D., 2015. Noradrenergic regulation of fear and drug-associated memory reconsolidation. Neuropsychopharmacology 40 (4), 793–803.
Overstreet, D.H., 2012. Modeling depression in animal models. Methods Mol. Biol. 829, 125–144.
Parsons, R.G., Ressler, K.J., 2013. Implications of memory modulation for post-traumatic stress and fear disorders. Nat. Neurosci. 16 (2), 146–153.
Pellow, S., Chopin, P., 1985. Validation of open:closed arm entries in an elevated plus-maze as a measure of anxiety in the rats. J. Neurosci. Methods 14 (3), 149–167.
Price, J.L., 2003. Comparative aspects of amygdala connectivity. Ann. N. Y. Acad. Sci. 985, 50–58.
Russo, S.J., Dietz, D.M., Dumitriu, D., Morrison, J.H., Malenka, R.C., Nestler, E.J., 2010. The addicted synapse: mechanisms of synaptic and structural plasticity in nucleus accumbens. Trends Neurosci. 33 (6), 267–276.
Salamone, J.D., Correa, M., Mingote, S.M., Weber, S.M., 2005. Beyond the reward hypothesis: alternative functions of nucleus accumbens dopamine. Curr. Opin. Pharmacol. 5 (1), 34–41.
Sandi, C., Haller, J., 2015. Stress and the social brain: behavioural effects and neurobiological mechanisms. Nat. Rev. Neurosci. 16 (5), 290–304.
Sandkuhler, J., Lee, J., 2013. How to erase memory traces of pain and fear. Trends Neurosci. 36 (6), 343–352.
Si, Y., Song, Z., Sun, X., Wang, J.H., 2018. microRNA and mRNA profiles in nucleus accumbens underlying depression versus resilience in response to chronic stress. Am. J. Med. Genet. Neuropsychiatr. Genet. 177 (6), 563–579.
Smoller, J.W., 2016. The genetics of stress-related disorders: PTSD, depression, and anxiety disorders. Neuropsychopharmacology 41 (1), 297–319.
Southwick, S.M., Charney, D.S., 2012. The science of resilience: implications for the prevention and treatment of depression. Science 338 (6103), 79–82.
Sun, X., Song, Z., Si, Y., Wang, J.H., 2018. microRNA and mRNA profiles in ventral tegmental area relevant to stress-induced depression and resilience. Prog. Neuro Psychopharmacol. Biol. Psychiatry 86, 150–165.
Sun, Y., Lu, W., Du, K., Wang, J.H., 2019. microRNA and mRNA profiles in the amygdala are relevant to fear memory induced by physical or psychological stress. J. Neurophysiol. 122 (3), 1002–1022. https://doi.org/10.1152/jn.00215.2019.
Sutoo, D., Akiyama, K., 2002. Neurochemical changes in mice following physical or psychological stress exposures. Behav. Brain Res. 134 (1–2), 347–354.
Thomas, K.L., Hall, J., Everitt, B.J., 2002. Cellular imaging with zif268 expression in the rat nucleus accumbens and frontal cortex further dissociates the neural pathways activated following the retrieval of contextual and cued fear memory. Eur. J. Neurosci. 16 (9), 1789–1796.
Thrall, G., Lane, D., Carroll, D., Lip, G.Y., 2007. A systematic review of the effects of acute psychological stress and physical activity on haemorheology, coagulation, fibrinolysis and platelet reactivity: implications for the pathogenesis of acute coronary syndromes. Thromb. Res. 120 (6), 819–847.
Toyoda, A., 2017. Social defeat models in animal science: what we have learned from rodent models. Anim. Sci. J. 88 (7), 944–952.
Tsankova, N.M., Berton, O., Renthal, W., Kumar, A., Neve, R.L., Nestler, E.J., 2006. Sustained hippocampal chromatin regulation in a mouse model of depression and antidepressant action. Nat. Neurosci. 9 (4), 519–525.
Tzschentke, T.M., Schmidt, W.J., 2000. Functional relationship among medial prefrontal cortex, nucleus accumbens, and ventral tegmental area in locomotion and reward. Crit. Rev. Neurobiol. 14 (2), 131–142.
Valinezhad Orang, A., Safaralizadeh, R., Kazemzadeh-Bavili, M., 2014. Mechanisms of miRNA-mediated gene regulation from common downregulation to mRNA-specific upregulation. Int. J. Genom. 970607 2014.

Vasconcelos, M., Stein, D.J., de Almeida, R.M., 2015. Social defeat protocol and relevant biomarkers, implications for stress response physiology, drug abuse, mood disorders and individual stress vulnerability: a systematic review of the last decade. Trends Psychiatry Psychother. 37 (2), 51–66.
Walf, A.A., Frye, C.A., 2007. The use of elevated plus maze as an assay of anxiety-related behavior in rodents. Nat. Protoc. 2 (2), 322–328.
Wang, D., Zhao, J., Gao, Z., Chen, N., Wen, B., Lu, W., Lei, Z., Chen, C., Liu, Y., Feng, J., Wang, J.H., 2015. Neurons in the barrel cortex turn into processing whisker and odor signals: a cellular mechanism for the storage and retrieval of associative signals. Front. Cell. Neurosci. 9, 320.
Wang, J.-H., 2019. Searching basic units of memory traces: associative memory cells. F1000Res. 8 (457), 1–28.
Wang, J.-H., Feng, J., Lu, W., Xiao, H., 2018. Prefrontal cortical neurons are recruited as secondary associative memory cells for associative memory and cognition. Biophys. J. 114 (3), 778–Pos.
Wang, J.-H., Lu, W., 2018. Molecular profiles in the brain are involved in fear memory induced by physical and psychological stress. 19. Soc. Neurosci. 425 (425) III61.
Wang, J.-H., Wang, D., Zhao, J., Gao, Z., 2013. Neurons in barrel cortex turn into processing whisker and odor signals: a novel form of associative learning. Soc. Neurosci. 653 14, WW11.
Wang, J.H., 2019a. Associative Memory Cells: Basic Units of Memory Trace, the first ed. Springer Nature, Springer.
Wang, J.H., 2019b. Searching basic units in memory traces: associative memory cells. F1000Res. 8, 457.
Wang, J.H., Cui, S., 2017. Associative memory cells: formation, function and perspective. F1000Res. 6, 283.
Wang, J.H., Cui, S., 2018. Associative memory cells and their working principle in the brain. F1000Res. 7, 108.
Wang, J.H., Feng, J., Xiao, H., Xu, Y., 2019. Secondary associative memory cells and their plasticity in the prefrontal cortex. Biophys. J. 116 (3), 427a.
Willner, P., Towell, A., Sampson, D., Sophokleous, S., Muscat, R., 1987. Reduction of sucrose preference by chronic unpredictable mild stress, and its restoration by a tricyclic antidepressant. Psychopharmacology (Berlin) 93 (3), 358–364.
Xu, A., Cui, S., Wang, J., 2015. Incoordination among subcellular compartments is associated to depression-like behavior induced by chronic mild stress. Int. J. Neuropsychopharmacol. 19 (5) pyv122.
Yang, F.C., Liang, K.C., 2014. Interactions of the dorsal hippocampus, medial prefrontal cortex and nucleus accumbens in formation of fear memory: difference in inhibitory avoidance learning and contextual fear conditioning. Neurobiol. Learn. Mem. 112, 186–194.
Zhang, F., Liu, B., Lei, Z., Wang, J., 2012. mGluR1,5 activation improves network asynchrony and GABAergic synapse attenuation in the amygdala: implication for anxiety-like behavior in DBA/2 mice. Mol. Brain 5 (1), 20.
Zhu, Z., Wang, G., Ma, K., Cui, S., Wang, J.H., 2017. GABAergic neurons in nucleus accumbens are correlated to resilience and vulnerability to chronic stress for major depression. Oncotarget 8 (22), 35933–35945.